AD 666769

DEVELOPMENT OF A FREE-FIELD SOIL STRESS GAGE FOR STATIC AND DYNAMIC MEASUREMENTS

by

J. K. Ingram

February 1968

D D C

MAR 26 1968

C

Sponsored by

Defense Atomic Support Agency

Conducted by

U. S. Army Engineer Waterways Experiment Station

CORPS OF ENGINEERS

Vicksburg, Mississippi

DEVELOPMENT OF A FREE-FIELD SOIL STRESS GAGE FOR STATIC AND DYNAMIC MEASUREMENTS

by

J. K. Ingram

February 1968

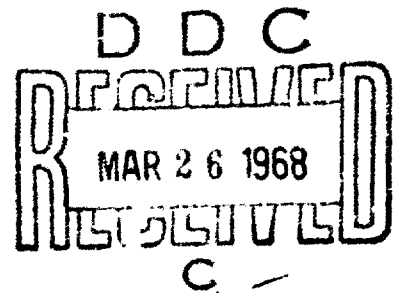Sponsored by

Defense Atomic Support Agency
NWER Subtask 13.503A

Conducted by

U. S. Army Engineer Waterways Experiment Station
CORPS OF ENGINEERS
Vicksburg, Mississippi

ABSTRACT

This report describes the development of three free-field soil stress gage types. One gage design, the sand dollar gage, was abandoned early in the investigation, while the other two, the W and SE gages, were subjected to various evaluation tests. Static and dynamic tests in sand and clay were conducted in the Waterways Experiment Station's Small Blast Load Generator (SBLG) at depths of burial up to 2-1/2 feet. The test soils and gage placement techniques used in the SBLG tests are described in Appendix B. The gages have been used in the laboratory evaluation of a cold gas loader and in two field tests: Operation Snowball, and a small energy-coupling-efficiency test conducted in 1965. Evaluation of the performance of the gages in these tests is presented in Appendix A.

The gages are rugged and relatively easy to place in the laboratory. They may be used for both static and dynamic measurements and have a linear pressure range from 1 to above 1,600 psi. The gages have very low acceleration sensitivity and hysteresis, and have excellent dynamic response capability--rise time less than 6 μsec and undamped natural frequency greater than 40 kHz. The temperature sensitivity (zero shift) of the gages is such that it will be of little consequence in dynamic tests and can be corrected

for in long-term static tests. Electrical sensitivity (as opposed to zero shift) remains essentially constant from -30 to 150 F. Of the two gage types discussed, the SE gage is recommended for use. It is much easier to place, is more rugged, and produces a cleaner dynamic signal than the W gage.

The gages can be calibrated to compensate for registration errors due to differences in soil and gage modulus; however, gage registration was found to be a function of placement method, depth of burial, input pressure, and conditions of the medium, not simply of modulus ratio. Where a minimum number of gages are to be used in sand, a dense tamping-in placement method is recommended for general use in laboratory tests. For tests in clay, the cut/no-cover method, in which the gage is placed in a matched cavity flush with the clay surface and covered in normal lifts, is recommended. Further investigation of field placement techniques is recommended.

PREFACE

This study was performed by the U. S. Army Engineer Waterways Experiment Station (WES) under the sponsorship of the Defense Atomic Support Agency (DASA) Nuclear Weapons Effects Test (NWET) Program as Subtask 13.503A, "Development and Evaluation of Stress and Motion Sensors."

The work was performed during the period 1962-1966 under the general supervision of Messrs. F. R. Brown and G. L. Arbuthnot, Jr., successive Chiefs of the Nuclear Weapons Effects Division, and L. F. Ingram, Chief of the Physical Sciences Branch. This report was written by Mr. J. K. Ingram under the direction of Mr. J. D. Day, Chief of the Blast and Shock Section.

The author wishes to acknowledge the assistance of the following individuals: Mr. J. T. Kitchens and Mr. J. V. Tarver, under the supervision of Mr. K. Daymond of the WES Instrumentation Branch for strain gaging and data retrieval, and Mr. J. T. Brogan and PVT T. Buckley of the Blast and Shock Section for assistance in data reduction and preparation.

COL Alex G. Sutton, Jr., CE, and COL John R. Oswalt, Jr., CE, were Directors of the WES during the study and the publication of this report. Mr. J. B. Tiffany was Technical Director.

CONTENTS

FIGURES

NOTATION

a   Radius of diaphragm, inches

c   Sonic velocity of the material, ft/sec

d   Flexural rigidity $= Eh^3/12(1 - v^2)$

D   Diameter, inches

e_o Output voltage, volts

E   Young's modulus (compression), psi

E_c Bulk modulus of gage (compression), psi

E_s Secant modulus of soil, psi

F   Gage factor

h   Diaphragm thickness, inches

H   Gage thickness, inches

K   Ratio of horizontal to vertical pressure over total cross-sectional area

L   Total gage thickness, inches

P_m Pressure indicated by gage, psi

P_{so} Applied surface pressure (to soil test sample), psi

P_1 Pressure at depth of interest

q   The intensity of a uniformly distributed load, psi

r   Distance from center of diaphragm

R   Electrical resistance, ohms

V   Input voltage, volts

Z   Depth of interest, inches

11

α Angle of friction between medium and chamber

δ Deflection of diaphragm, inches

ΔR Change in resistance, ohms

ϵ Strain, in/in

λ_D Scaled charge depth, $ft/lb^{1/3}$

λ_r Scaled radial distance from charge, $ft/lb^{1/3}$

λ_R Scaled radial distance, $ft/lb^{1/3}$

ρ Mass density, lb/ft^3

σ Stress, psi

σ_c Stress at center of diaphragm, psi

σ_r Radial stress in diaphragm, psi

σ_t Tangential stress in diaphragm, psi

υ Poisson's ratio, coefficient of friction between medium and chamber, $\tan \alpha$

CONVERSION FACTORS, BRITISH TO METRIC UNITS OF MEASUREMENT

Multiply	By	To Obtain
QUANTITIES AND UNITS OF SPACE		
Length		
Inches	2.54 (exactly)	Centimeters
Feet	0.3048 (exactly)	Meters
Yards	0.9144 (exactly)	Meters
Miles (statute)	1.609344 (exactly)	Kilometers
Area		
Square inches	6.4516 (exactly)	Square centimeters
Square feet	0.092903 (exactly)	Square meters
Square yards	0.836127	Square meters
Square miles	2.58999	Square kilometers
Volume[a]		
Cubic inches	16.3871	Cubic centimeters
Cubic feet	0.0283168	Cubic meters
Cubic yards	0.764555	Cubic meters
Capacity[a]		
Fluid ounces (U.S.)	29.5737	Cubic centimeters
	29.5729	Milliliters[a]
Liquid pints (U.S.)	0.473179	Cubic decimeters
	0.473166	Liters[a]
Gallons (U.S.)	3.78543	Cubic decimeters
	3.78533	Liters[a]
Gallons (U.K.)	4.54609	Cubic decimeters
	4.54596	Liters[a]
Cubic feet	28.3160	Liters[a]
QUANTITIES AND UNITS OF MECHANICS		
Mass		
Grains (1/7000 lb avdp)	64.79891 (exactly)	Milligrams
Troy ounces (480 grains)	31.1035	Grams
Ounces (avdp)	28.3495	Grams
Pounds (avdp)	0.45359237 (exactly)	Kilograms
Short tons (2000 lb)	907.185	Kilograms
	0.907185	Metric tons
Long tons (2240 lb)	1016.05	Kilograms
Force/Area		
Pounds per square inch	0.070307	Kilograms per square centimeter
	0.689476	Newtons per square centimeter
Pounds per square foot	4.88243	Kilograms per square meter
	47.8803	Newtons per square meter
Mass/Volume (Density)		
Ounces per cubic inch	1.72999	Grams per cubic centimeter
Pounds per cubic foot	16.0185	Kilograms per cubic meter
	0.0160185	Grams per cubic centimeter
Tons (long) per cubic yard	1.32894	Grams per cubic centimeter
Mass/Capacity		
Ounces per gallon (U.S.)	7.4893	Grams per liter[a]
Ounces per gallon (U.K.)	6.2362	Grams per liter[a]
Pounds per gallon (U.S.)	119.829	Grams per liter[a]
Pounds per gallon (U.K.)	99.779	Grams per liter[a]
Bending Moment or Torque		
Inch-pounds	0.011521	Meter-kilograms
	1.12985×10^6	Centimeter-dynes
Foot-pounds	0.138255	Meter-kilograms
	1.35582×10^7	Centimeter-dynes
Foot-pounds per inch	5.4431	Centimeter-kilograms per centimeter
Ounce-inches	72.008	Gram-centimeters
Velocity		
Feet per second	30.48 (exactly)	Centimeters per second
Miles per hour	1.609344 (exactly)	Kilometers per hour
	0.44704 (exactly)	Meters per second
Flow		
Cubic feet per minute	0.4719	Liters[a] per second
Gallons (U.S.) per minute	0.06309	Liters[a] per second

[a] Laboratory volumetric apparatus in the United States is calibrated in milliliters rather than cubic centimeters (1 ml = 1.000028 cm^3). The difference (28 ppm) is seldom of consequence.

CHAPTER 1

INTRODUCTION

1.1 OBJECTIVE

This investigation was part of a continuing program to develop
reliable instrumentation for measuring static and dynamic soil
stress both in the free-field and at boundary interfaces. The
overall objective was to develop capable instruments and to
evaluate them under realistic conditions. The specific objective
of this study was to develop and evaluate a free-field soil stress
gage capable of working in both static and dynamic environments.

1.2 SCOPE

This report describes the design approach and assembly tech-
niques employed in the development of three free-field stress gage
types. One gage design was abandoned early in the investigation,
while the other two were subjected to various evaluation tests.
Fluid and mechanical calibrations were conducted to pressure levels
up to 1,800 psi.[1] Typical gages were tested in a shock tube for
dynamic response and on a drop table for acceleration sensitivity.
Thermal effects on gage output were studied in a temperature range

---

[1] A table of factors for converting British units of measurement
to metric units is presented on page 13.

of -30 to 150 F. Static and dynamic tests in sand and clay were
conducted in the Waterways Experiment Station's Small Blast Load
Generator (SBLG) Facility at depths of burial up to 2-1/2 feet. The
sand and clay and the gage placement techniques used in the SBLG
tests are described in Appendix B. The gages have been used in the
laboratory in the evaluation of a cold gas loader and in two field
tests: Operation Snowball (Reference 1) and a small energy-coupling-
efficiency test conducted in 1965. Evaluation of the performance of
the gages in these tests is presented in detail in Appendix A.

1.3 BACKGROUND

1.3.1 Soil Stress. The presence of an inclusion such as a
gage in a granular medium disrupts the stress field, causing either
stress concentrations or stress reliefs depending on whether the
inclusion is more or less stiff than the medium. This stress
mobilization has been termed soil arching, further defined as pas-
sive arching when the soil deforms more than the gage and active
arching when the gage deforms more than the soil. Arching can
seriously affect gage output; ideally, therefore, a gage that is to
be placed in a soil mass should have the same deformation charac-
teristics as the soil it replaces. Because of the wide variation
of soil properties and the requirement for dynamic response, it is
not practical to consider precise matching of the gage to all media.

1.3.2 Experimental Investigations. An extensive gage study
was conducted by the U. S. Army Engineer Waterways Experiment
Station (WES) in the 1940's (Reference 2). Flat, disk-shaped gages
placed within a sand mass were found to have an essentially constant
change in gage output with changes in compressibility when the ratio
of the gage diameter to deflection was greater than 2,000. Pressure
errors indicated by the gages were also found to be constant for
diameter-to-thickness ratios greater than 5. The indicated pres-
sures were found to be approximately 100 to 150 percent of applied
static surface pressures for both conditions.

Reference 3, a report of experiments with diaphragm gages,
confirmed the WES findings, and concluded that a gage design should
incorporate stiff, annular rings supporting a stiff diaphragm.

In Reference 4 (1954) formulas developed by WES were used to
compute pressure errors of buried gages of varying aspect (diameter-
to-thickness) ratios with elastic moduli between 2 and 100 times
that of a sand (Figure 1.1). Where the aspect ratio was 5 or
greater, the gage-pressure error varied linearly.

In Reference 5 and later in Reference 6, the compressibility
effect was considered as a problem of an elastic disk embedded in an
elastic medium. In Reference 6, pressure distributions across the
faces of gages buried in a homogeneous solid were also investigated.
It was determined that the pressure field rises near the gage

16

perimeter and decreases toward the center (Figure 1.2). This effect suggests that pressure errors would be greater if the sensing area of the gage comprised the entire gage face than if only the central portion of the face were active. This hypothesis was experimentally confirmed in Reference 4. Figure 1.3 is a graphical presentation of the effects of stiffness ratio and pressure distribution on registration error.

Based on the foregoing studies, it is reasonable to infer that a gage can be designed to measure static pressures with a relatively constant error; that is, a constant ratio of measured pressure P_m to applied pressure P_{so} regardless of changes in soil moduli.

For the gage to be useful as a dynamic sensor, it should have a fast response (in the microsecond range) and a high natural frequency. The gage should also be acoustically matched to the medium in which it is contained. The acoustic impedance is the product of the density and the acoustic velocity of a material. Of these two factors, the acoustic velocity is the most difficult to incorporate in a gage.

1.3.3 Early Developmental Gages. Numerous gages incorporating some or most of the desired design features have been developed (References 7, 8, and 9), but all have had their limitations. Piezoelectric gages, which are reasonably adequate for dynamic measurements, are not well adapted for static or near-static

17

measurements. They are usually heat sensitive and their charge-
sensitivity may vary with the applied stress level (as in several
artificial ceramic materials).
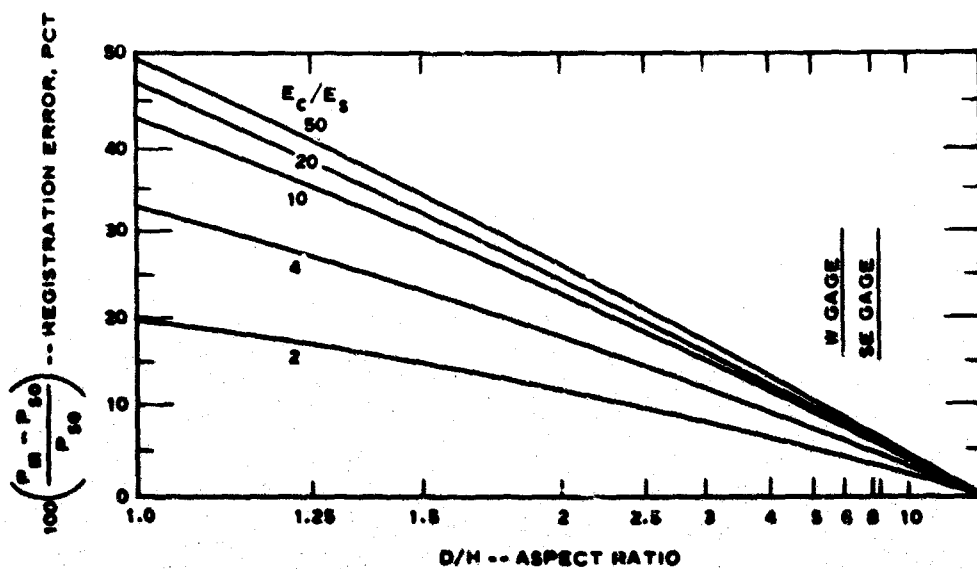
Figure 1.1 Variation of error with aspect ratio D/H and stiffness ratio E_c/E_s (Reference 4).
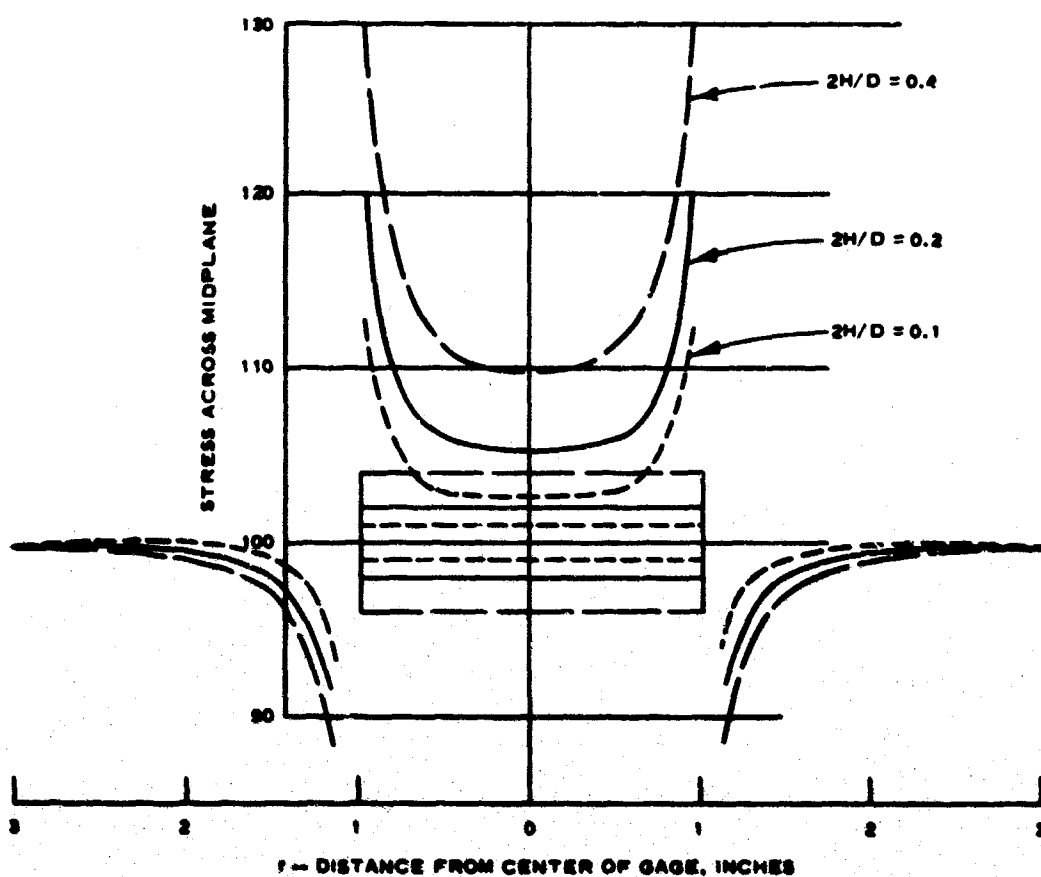
Figure 1.2 Effect of gage aspect ratio on stress
distribution (Reference 6).
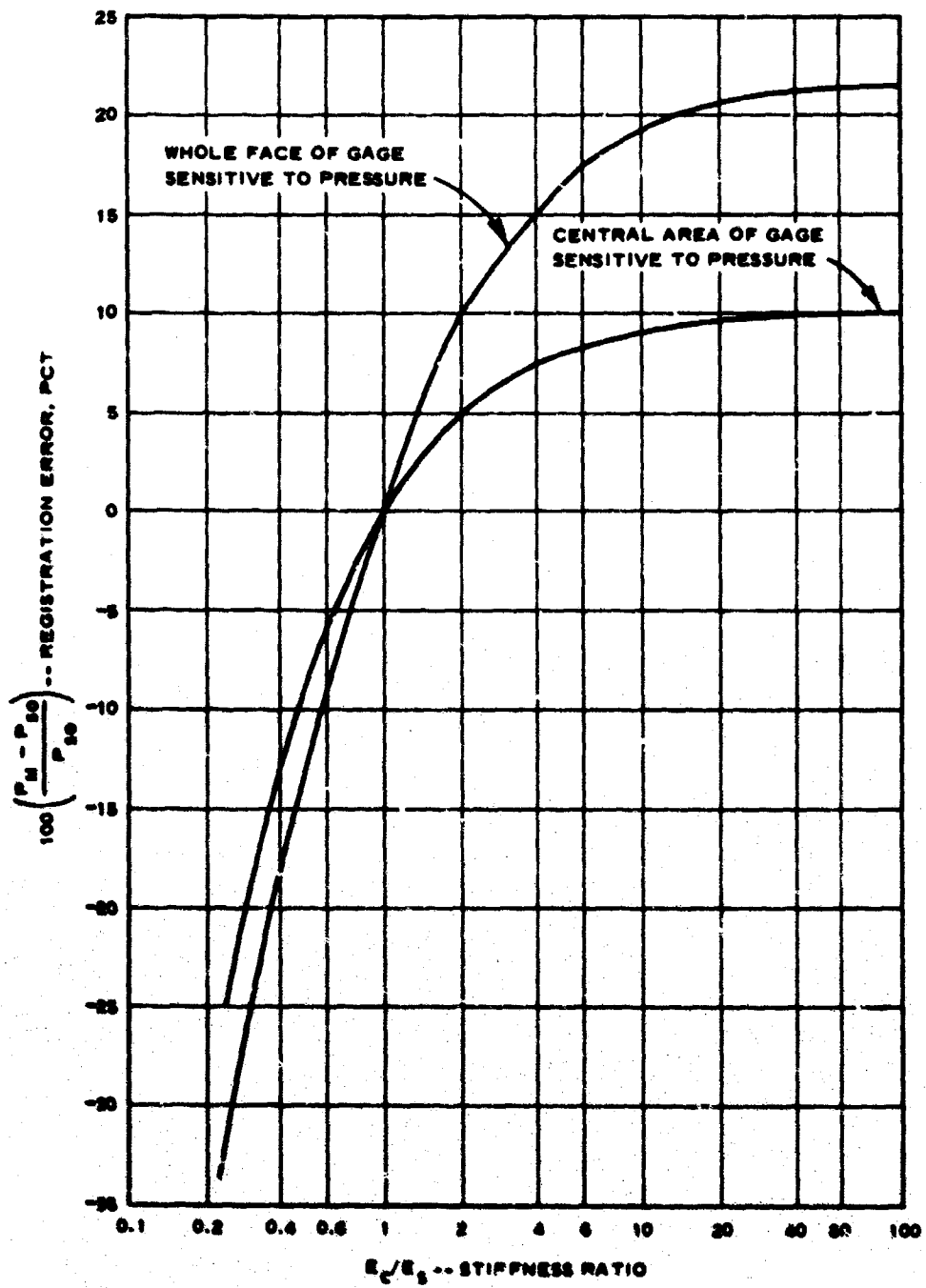
Figure 1.3 Variation of error of gage with stiffness ratio for D/H = 5 (Reference 6).

CHAPTER 2

DESIGN

2.1 APPROACH

The approach adopted was based on the assumption that, although a very stiff gage (as compared to the soil) would indicate greater pressures than were applied, the overregistration would be predictable (by laboratory calibration) and would be essentially constant for any conceivable soil modulus. Moreover, a stiff gage is inherently able to respond to rapid pressure changes because of its higher natural frequency; thus, good dynamic response was expected also. The primary design guides are (1) wafer shape with an aspect (D/d) ratio greater than 5, (2) diameter-to-deflection ratio greater than 2,000, (3) high gage modulus as compared to soil, (4) only the central portions of the gage surfaces active, (5) density matched to the medium, (6) small physical size, and (7) static and dynamic measuring capability with remote electronic readout.

Of the possible gage designs considered, two showed promise. A design based on the load column principle was investigated, but, primarily due to size requirements, was not pursued in depth. The design adopted was that of a deflecting, flat, circular diaphragm with rigidly clamped edges. Strains induced into the diaphragm by an external stress were sensed by solid-state strain gages which were bonded to the diaphragm.

22

2.2 DESIGN EQUATIONS

General design equations were adopted from Reference 10 and are presented in this section.

2.2.1 Assumed Conditions. The acting member is a flat, circular plate (diaphragm) with rigidly clamped edges. The design pressure was set at 500 psig based on anticipated survival from realistic loadings of medium yield weapons. The diaphragm diameters were set for practical handling and strain gaging in actual assembly. The maximum allowable center deflections at the design pressure were set at a level that would produce high enough strains for a resolution of 1 psi. The other attendant parameters were calculated from these set conditions.

2.2.2 Maximum Center Deflection and Modulus of Compressibility. The equation for maximum center deflection of a circular diaphragm of rigidly fixed edges is given as

$$\delta = \frac{qa^4}{64d} \tag{2.1}$$

where q = the intensity of a uniformly distributed load, psi

a = radius of diaphragm, inches

d = flexural rigidity = $\dfrac{Eh^3}{12(1 - v^2)}$

E = Young's modulus for the material, psi

h = Diaphragm thickness, inches

v = Poisson's ratio, dimensionless

23

If Equation 2.1 is solved for h , the relation becomes

$$h = \sqrt[3]{\frac{12qa^4 (1 - v^2)}{64E\delta}} \qquad (2.2)$$

To determine the modulus of compressibility E_c of the gage, based on the maximum center deflection, we utilize the stress-strain relation

$$E_c = \frac{\sigma}{\epsilon}$$

where σ = design soil stress = 500 psig

For a single diaphragm

$$\epsilon = \frac{\delta}{L} \qquad (2.3)$$

where L is the total gage thickness

Thus, the equation becomes

$$E_c = \frac{\sigma}{\frac{\delta}{L}} \qquad (2.4)$$

And for a symmetrical transducer with two deflecting diaphragms

$$E_c = \frac{\sigma}{\frac{2\delta}{L}} \qquad (2.5)$$

2.2.3 Stress at Center of Diaphragm. It can be seen from Figure 2.1 that, at the center of the diaphragm

$$\sigma_c = \sigma_r = \sigma_t = \frac{3(1 + v) qa^2}{8h^2} \qquad (2.6)$$

24

where σ_c = stress at center of diaphragm

σ_r = radial stress

σ_t = tangential stress

2.2.4 <u>Strain at Center of Diaphragm</u>. The strain ϵ_c at the center of the diaphragm is given by

$$\epsilon_c = \frac{\sigma_c}{E} \tag{2.7}$$

For the diaphragm gage, four active strain gages are used in a full bridge circuit. For maximum output, two gages must be in compression and two in tension. The tension gages are located in the center of the diaphragms (see Figure 2.1) where the radial stress is

$$\sigma_r = \frac{3(1 - \upsilon)\ qa^2}{8h^2} \tag{2.8}$$

Since it was not possible to place a strain gage exactly at the outer edge of the diaphragm in the region of maximum compressive strain, the gage is placed at $r = 0.827a$ where the radial stress is equal to approximately one-half the edge condition, or

$$\frac{1}{2}\left(- \frac{3}{4} \frac{qa^2}{h^2}\right) = - \frac{3}{8}\left(\frac{qa^2}{h^2}\right) \tag{2.9}$$

The strains at these gage locations can be computed from the stresses and Young's modulus of the gage material (see Figure 2.1).

Knowing the sensitivity (gage factor) of the strain gages, it is possible to predict the output voltage of the strain gage bridge

25

for given stresses on the gage and bridge input voltages. This procedure is discussed in the next section.

The advent of piezoresistive strain gages with sensitivities up to 60 times those of conventional strain gages has made it possible to use very small diaphragm deflections. By restricting the total gage deformation to a very small value, a high gage modulus can be achieved. The resulting gage should be stable and should produce repeatable measurements. The use of piezoresistive elements also allows the resolution of both static and dynamic stresses.

2.3 ELECTRICAL CONSIDERATIONS

According to Reference 11, the use of a Wheatstone bridge has two advantages. First, it provides nominal temperature compensation, provided that all gages are electrically equal and mounted on the same base material. Temperature compensation can become a critical factor in long-term static measurements. Second, an increase in sensitivity can be attained since all strain gages are active sensors. The signal from the two compression gages (R_2 and R_4 of Figure 2.2) is added to the signal from the tension gages (R_1 and R_3) to give optimum sensitivity.

The output signal e_o from a bridge circuit using all active elements can be calculated from the following equation from Reference 11:

26

$$e_o = \frac{VR_g}{4(R + R_g)} \left[\frac{\Delta R_1}{R_1} - \frac{\Delta R_2}{R_2} + \frac{\Delta R_3}{R_3} - \frac{\Delta R_4}{R_4} \right] \tag{2.10}$$

where V = input, volts

R_g = resistance of readout device, ohms

R = nominal gage resistance, ohms

ΔR_1 = change in electrical resistance of gage 1

R_1 = electrical resistance of gage 1

where all four gages have nominal unstrained resistances equal to R .

It can be seen from Equation 2.10 that if gages R_2 and R_4 are subjected to strains of the same magnitude as, but of opposite sign from those of R_1 and R_3 ,

$$e_o = \frac{VR_g}{4(R + R_g)} \frac{(4\Delta R)}{R} = \frac{VF\epsilon R_g}{R + R_g} \tag{2.11}$$

The output voltage for $R_g = \infty$ is obtained by taking the limit of e_o as R_g approaches ∞ .

$$e_o = \lim_{R_g \to \infty} e_o = \frac{\frac{d}{dR_g}(VF\epsilon R_g)}{\frac{d}{dR_g}(R + R_g)} = VF\epsilon \tag{2.12}$$

The specific output for the bridge then becomes

$$\frac{e_o}{V} = F\epsilon \tag{2.13}$$

27
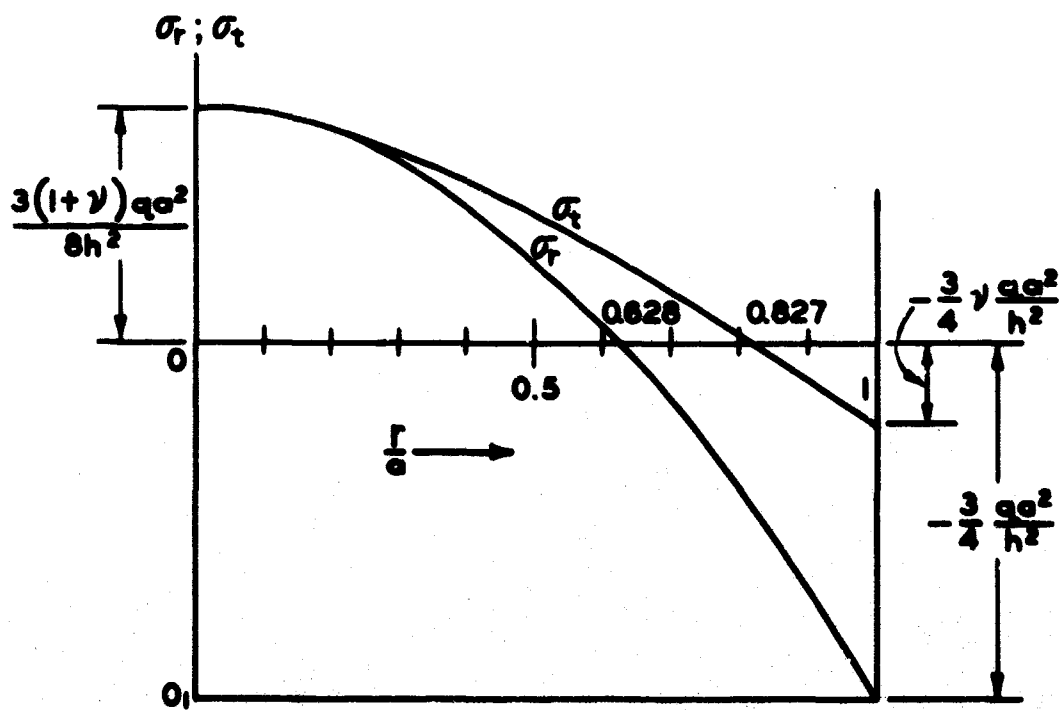
Figure 2.1 Stress distribution in a uniformly loaded
diaphragm with clamped edges (Reference 10).
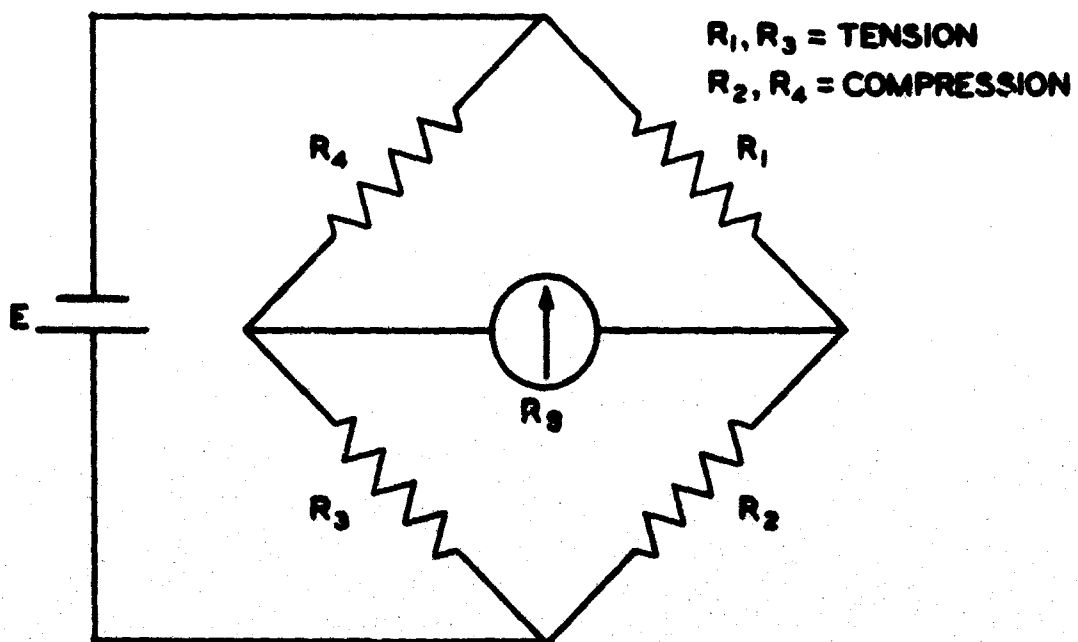
Figure 2.2 Gage electrical circuit.

R$_1$, R$_3$ = TENSION
R$_2$, R$_4$ = COMPRESSION

29

CHAPTER 3

TRANSDUCER DEVELOPMENT

3.1 SAND DOLLAR GAGE

The first developmental gage was dubbed "sand dollar" because its physical appearance so closely resembled the sea urchin of the same name (Figure 3.1). The gage consists essentially of a single stainless steel diaphragm with rigid sidewalls set in a tapered Plexiglas baffle. Two strain gages were bonded on the diaphragm near the center and two radially near the periphery. Gage parameters are given in Table 3.1.

The gage showed good linearity to fluid calibrations, but was found to be quite sensitive to bending moments around the Plexiglas baffle.

Although some good experience in gaging techniques was obtained with this gage, its design was abandoned in an effort to eliminate the edge effects and to make a more rugged gage.

3.2 W AND SE GAGES

In order to obtain the best average sampling of the stress field it was felt desirable to provide active sensing in both top and bottom surfaces of the proposed transducer. Very stiff sidewalls are required to minimize bending as well as lateral sensitivity in the gage. The gage must also be matched to the soil

30

density for proper dynamic response.

Two sizes of gages were developed under this study. The first, the W gage, is 3 inches in diameter and 1/2 inch thick (Figure 3.2). The second, the SE gage, is 2 inches in diameter and 0.226 inch thick (Figure 3.3).

The basic sensing unit for both gages is a wafer-shaped metal housing with very stiff sidewalls containing machined diaphragms in both top and bottom surfaces. The general design equations were given previously in Section 2.2. The sensing unit is surrounded by a plastic baffle to provide the required aspect ratio and proper density matching. Two P-type, silicon, solid-state strain gages are attached to each diaphragm (one in the center and one near the edge) with epoxy-resin cement and electrically connected as a half bridge, the final assembly being connected as a full bridge.

The use of a small transducer is desirable because of the size limitations of most laboratory test chambers. The size requirement becomes most obvious if the gages are used in small chambers for stress measurements in the vicinity of model structures where the interaction effects between gage and structure must be taken into consideration.

The experience gained during the construction of several 3-inch-diameter (W-type) gages indicated that a smaller gage could easily be made. A one-third size reduction was successfully

31

produced and several other refinements were incorporated in the SE

gage design. A detailed assembly procedure for this gage is given

in Reference 12. The basic housing was fabricated from stainless

steel to increase the gage's ruggedness and to minimize any reaction

with the environment. The SE gage was found to be considerably

easier to place in a soil specimen and had better dynamic response

than the larger model. It is considered the most satisfactory de-

sign of this investigation. Several gages of each size were con-

structed for evaluation purposes. Some characteristics of both gage

types are listed in Table 3.1.

TABLE 1.2 GAGE PARAMETERS

	Aperture Parameters			Gage Parameters						
Material	Diameter	Thickness	Diameter/Deflection Ratio	Diameter	Thickness	Diameter/Thickness Ratio	Modulus E_c	Natural Frequency	Apparent[a] Strain Sensitivity	Specific Output e_o
	inch	inch		inch	inch		psi	kHz	$\mu\epsilon$/psi	mv/v/psi
Most Dollar:										
Reinforced steel	1.35	0.054	1.000	2.2	0.400	8.0	1.25×10^5	30	30	0.080
Aluminum	1.52	0.14	8.000	2.0	0.500	0.9	1.00×10^6	40	20	0.010-0.014
Stainless steel			4.000	2.0	0.226	8.8	4.52×10^5	40	20	0.017-0.020

[a] Used with strain indicator with gage factor dial setting of 2.0.

33
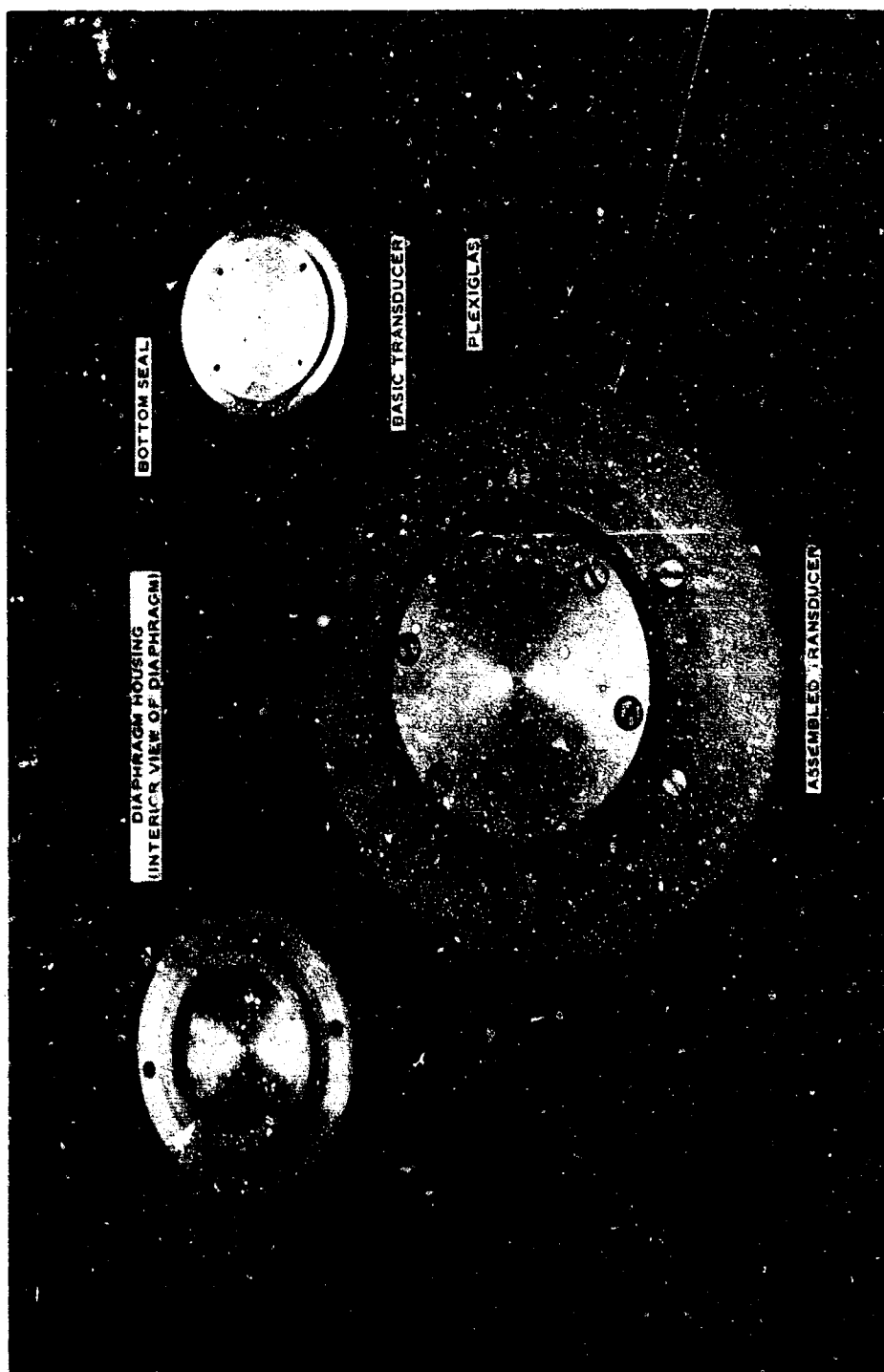
Figure 3.1 Sand dollar gage.

45° TYP

1.500 DIA

A

A

PLAN

LEGEND

MATERIALS:

TYPE 2024-T4 ALUMINUM

PLEXIGLAS

3.000

1.750

0.750

0.906

0.162

0.800

0.162

0.234

CONNECTOR-GLENITE C30-RI-4-HT
DRILL 3/8 HOLE × 0.234 DEEP

3/16 ALUMINUM TUBING

0.223 - 1/8 ∅ HOLE

0.125 TUBE INSET

1.000

1.250

SECTION A-A
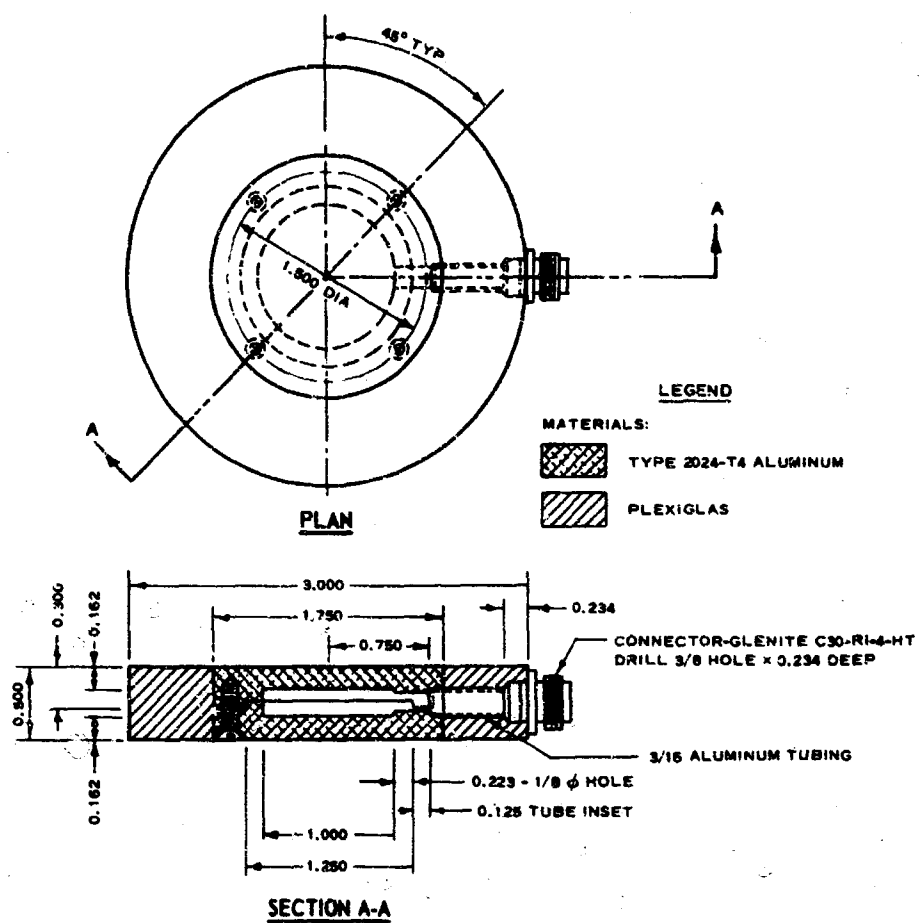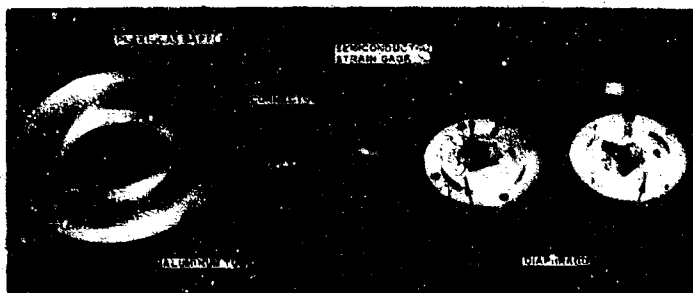
a. Schematic.

b. Disassembled view.

c. Assembled view.

Figure 3.2 W soil stress gage. Dimensions, except angle,
are in inches.

LEGEND

▨ TYPE 416 STAINLESS STEEL

▨ EPOXY RESIN

PLAN

SECTION AA
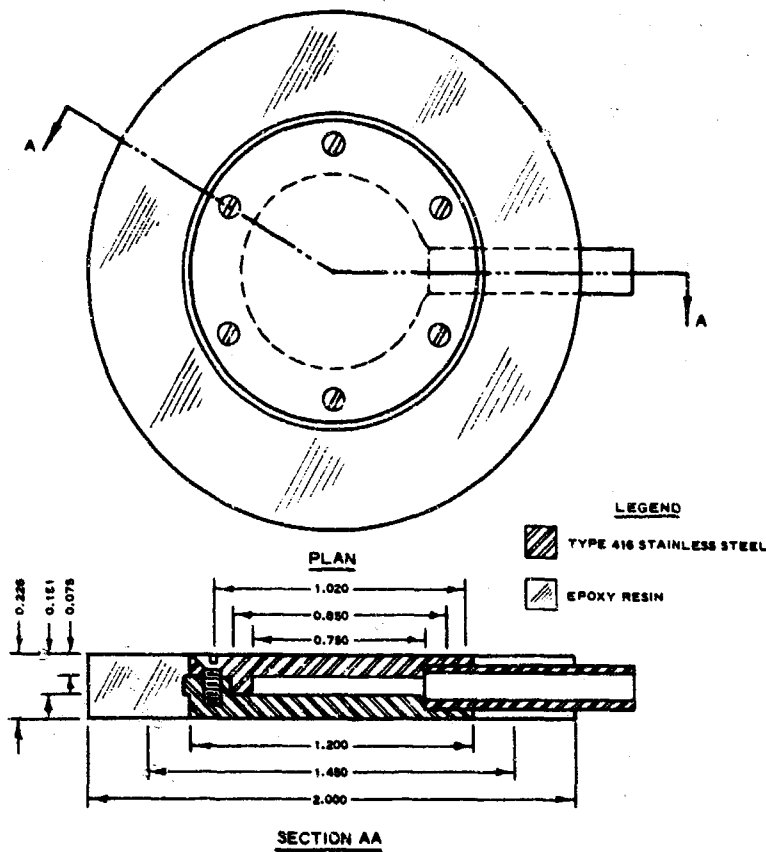
a.   Schematic.

b.   Disassembled view.
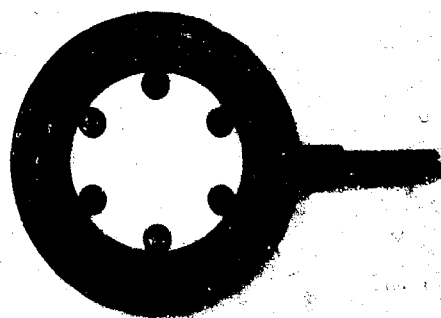
c.   Assembled view.

Figure 3.3   SE soil stress gage.   Dimensions are in inches.

CHAPTER 4

GAGE EVALUATION

4.1 FLUID CALIBRATION

All gages were statically calibrated in a small chamber using compressed nitrogen. Tests were made (1) with the nitrogen completely surrounding the gages, and (2) with the pressure applied only to the sensing surfaces through rubber diaphragms. No significant differences were observed between these two methods. The responses of the gages were linear to above 600 psi and exhibited little hysteresis (Figure 4.1a). One gage calibrated linearly to 1,800 psi.

4.2 DYNAMIC RESPONSE

Both W and SE gages were subjected to side-on step shock waves in a shock tube to determine dynamic response to a known input. A typical oscillograph record is shown in Figure 4.1b. These tests showed the rise time to be less than 6 μsec and the natural frequency to be greater than 40 kHz for both gages. These results are considered excellent since under normal conditions of intended use (buried in soil) the response requirements are much less severe than the response requirements for an air-shock measurement; therefore, the gages can be used to measure dynamic pressures in soil with confidence in gage response.

4.3 DROP-TABLE TESTS

Drop-table tests were made to determine acceleration sensitivity. Figure 4.2a shows the test setup. The gages were attached to the traveling stage of the drop table so that the direction of travel was normal to the gage diaphragms. A square-wave acceleration pulse of about 7-msec duration was applied to the table and monitored with a standard accelerometer. These tests showed that for accelerations up to about 90 g the gage acceleration sensitivity was less than 0.04 psig. A typical SE gage drop-test record is shown in Figure 4.2b.

4.4 THERMAL SENSITIVITY

Thermal effects on the SE and W gages were evaluated for a temperature range of -30 to 150 F. The gages were found to have a thermal sensitivity (base line shift) equivalent to <1 psi/F. Although the gages are fairly sensitive to temperature, even under adverse temperature conditions the gage temperature will rise only a few degrees in the short duration of the pressure pulse of a dynamic test. When long-term static tests are involved, the soil temperature remains relatively constant at depth. The temperatures can be monitored, and corrections made if required. Electrical sensitivity was found to be essentially constant down to the lower test limit of -30 F.

4.5   LABORATORY TESTS IN SOIL

Several pilot tests were conducted on both W and SE gages in dense, dry sand (Reference 13). These tests showed the gages to overregister for both static and dynamic loadings, but also showed noticeable scatter in data between the gage types. Based on these results, a more comprehensive series of static and dynamic evalua- tions, reported in detail in Appendix A, was made with close atten- tion given to controls on soil and gage placement. Two types of soil were used, two medium to fine, well-graded dry sands and a stiff, cohesive clay. A description of the soils is given in Appendix B.

4.5.1   Test Equipment. The laboratory evaluations were made in the Small Blast Load Generator (SBLG). This chamber, described in Reference 14, is composed of different-size rings and bases which permit the height to be altered, and has means of loading the soil surface both statically and dynamically. Static loads are applied using compressed gas, separated from the soil surface by a membrane. Dynamic loads are applied to the surface by detonating explosives in a specially designed lid. The tests discussed in this report were conducted in the long soil column base, better known as the "infinite base," and the rigid concrete base.

Static surface loading pressures were measured with a Bourdon- type mechanical gage, and dynamic pressures were measured with a

39

commercial fluid pressure transducer (Norwood Model 211). Dynamic
gage signals were conditioned and amplified through a dc analog
amplifier system and recorded on a light-beam galvanometer oscil-
lograph.

In addition to the study of depth effects, numerous measure-
ments were made with SE gages mounted flush with the surface of a
sand in a 10-inch-diameter, dynamic gas loading device.

4.5.2 Gage Placement Methods. Three methods of gage place-
ment in a sand specimen were evaluated:

1. Tamping-in method: a dense placement where gage was tamped
into the sand (Method I).

2. Raised-mound method: a dense placement where gage was
placed in a tamped excavation, covered (mounded) over with sand,
and sand was tamped (Method II).

3. Set-on-surface method: a loose placement where gage was
simply set on sand and additional sand was sprinkled on to complete
cover (Method III).

Three methods of gage placement in a clay were also investigated:

1. Cut/no-cover method: gage placed in an exact excavation
(Method C-I).

2. Cut-and-cover method: gage placed as in Method C-I, but a
mound of clay placed over gage and hand-tamped (Method C-II).

3. Deep-cut-and-backfill method: gage placed in a deep cut

in the clay and cut backfilled (Method C-III).

A detailed description of the placement techniques is given in Appendix B.

4.5.3 Tests Conducted. The first series of tests, six 500-psi static load cycles and two 250-psi dynamic load cycles at each of five depths of burial, was conducted in an unlined sand specimen in the infinite base SBLG. The remaining tests, a series of six 300-psi static load cycles and one 150-psi dynamic load cycle for each placement method in both sand and clay, were conducted in the concrete base SBLG with a grease-neoprene sidewall-friction-reducing liner (References 15 and 16). Both W and SE gages were used in the first series of tests; only SE gages in the remainder.

4.5.4 Results. General observations on gage performance are presented in this section. Appendix A gives a detailed treatment of the test results.

Gage registrations were found to be a function of placement, depth of burial, input (applied surface) pressure, and condition of the medium (i.e. virgin or preloaded), and not merely a simple matter of moduli ratios. Gage response was predictable at burial depths greater than one gage diameter (2 inches for the SE gages). The gages gave excellent results when flush-mounted with the specimen surface; however, at burial depths less than one gage diameter the registration was somewhat erratic. Generally, scatter and

registration were observed to decrease with increasing pressure and medium compaction.

Minimum average static registration error for a gage array in sand was achieved with the simple set-on-surface method of placement. However, considerable scatter was evident in the data. This suggests that several gages should be employed for a given location to afford maximum confidence in the data when this placement technique is used. The tamping-in method gave a relatively high gage registration (about 25 percent for both static and dynamic tests) but less data scatter. This placement method was both consistent and repeatable and supports the basic design concepts. It is recommended for general laboratory testing in sand.

Flush-mounted gages performed extremely well at both 1,000- and 2,300-psi loadings. Surface pressure waveforms and amplitudes were in good agreement with the measured gas pressure regime. A 10 percent high surface pressure measurement was noted at 1,000 psi, but an equal reading was observed at the 2,300-psi loading.

Results in clay revealed that the most satisfactory placement was achieved with the cut/no-cover method. The gages were found to underregister by about 8 percent statically and overregister by 3 to 4 percent dynamically.

4.6 FIELD TESTS

Several gages were used to measure earth stress to a depth of 12 feet in the 1964 Snowball experiment (Reference 1). The gages were placed in a sand-filled borehole located at the 300-psi surface overpressure region. The general performance of the gages was satisfactory. The wave shapes showed amplitude attenuation and rise time increase with increasing depth. With the exception of the shallowest (0.5-foot) gage, the measured amplitudes appeared reasonable.

A small-scale test using buried 2-pound, spherical TNT charges was conducted at the WES in 1965. Stress gages were placed in the ground (a silty loess) at varying radii. Recorded stress waveforms from the directly coupled energy were of excellent quality. Stresses computed from measured particle velocity compared favorably with the measured stresses.
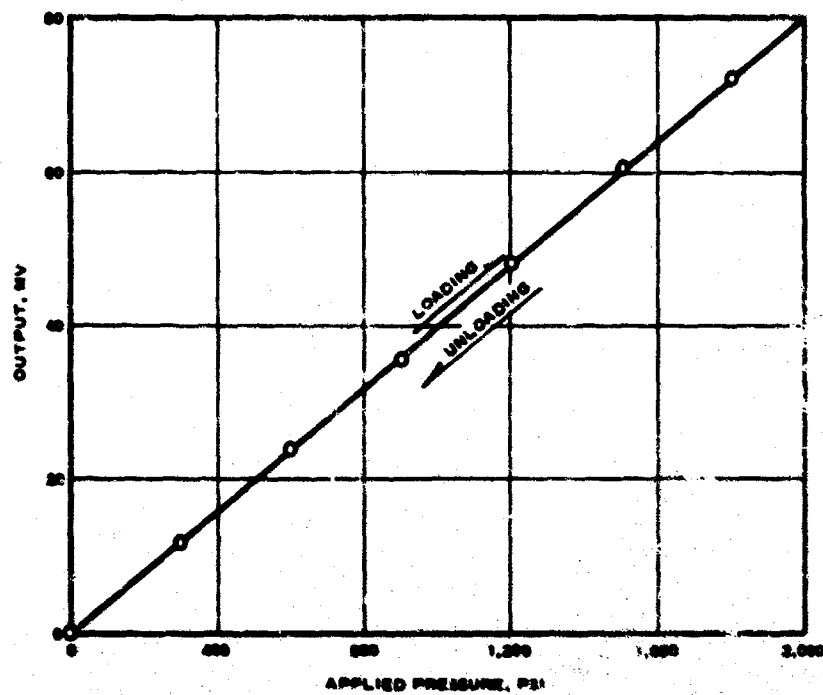
a. Typical fluid calibration curve
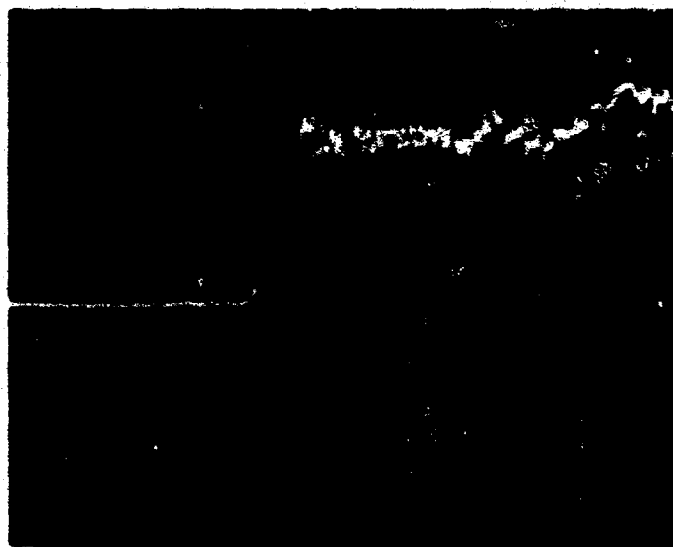
b. Gage response to a step air shock.

Figure 4.1 Typical 3E gage static and dynamic response.
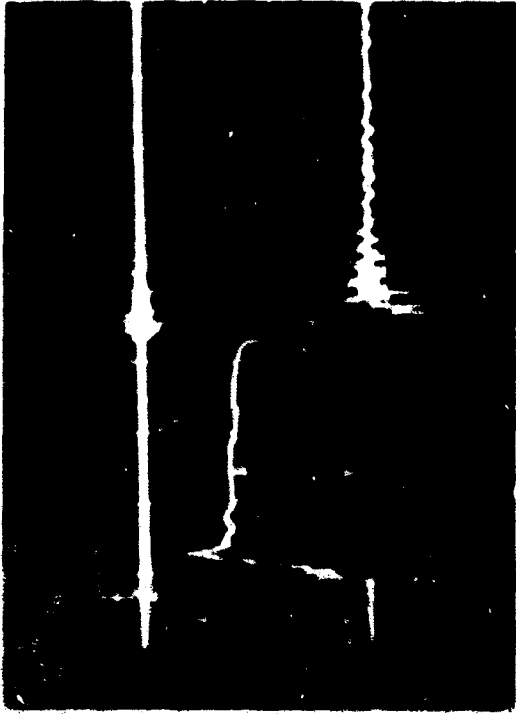
b. SE gage drop-test record.

a. Drop table.

Figure 4.2 Acceleration sensitivity test on SE gage.

45

CHAPTER 5

CONCLUSIONS AND RECOMMENDATIONS

5.1 CONCLUSIONS

The goal of this study was to develop soil pressure gages for use in both static and dynamic environments. The gages developed embody the physical characteristics required to ensure the most repeatable performance in soils; that is, they are small, thin, symmetrical, wafer-shaped gages having an aspect ratio greater than 5, their diameter-to-deflection ratio is greater than 2,000, only the central portions of the faces are active, and the gage density is approximately that of soil.

Gage registrations were found to be a function of placement, depth of burial, input pressure, and condition of medium (i.e. virgin or preloaded), and not simply a matter of moduli ratios.

The gages are stiffer than soil and therefore will generally overregister in coarse granular materials because of passive arching; however, this overregistration is repeatable for a given placement technique, and the gages can be calibrated accordingly. The arching problem is considerably less in clayey soils. The gages are rugged and relatively easy to place in the laboratory; these qualities are essential. The design assumptions have been substantially proven in laboratory and field testing.

The gages can be used for both static and dynamic measure-
ments, and have a pressure range from 1 to about 2,000 psi. The
linear range of the gages exceeds 1,800 psi. The gages have very
low acceleration sensitivity and hysteresis, and have excellent
dynamic response capability--rise time less than 6 μsec and un-
damped natural frequency greater than 40 kHz.

The gages do show temperature sensitivity (zero shift); how-
ever, this sensitivity is generally much less than for most piezo-
electric devices. The temperature sensitivity is of little conse-
quence for dynamic tests with buried gages and can be corrected
for in long-term static tests. Electrical sensitivity (as opposed
to zero shift) remains essentially constant over the range -30 to
150 F.

5.2 RECOMMENDATIONS

The gages have been thoroughly evaluated in dry sand and
clay in the laboratory, and in limited field operations, and are
currently being used routinely in both laboratory and field testing
by the WES.

Of the two types (SE and W) discussed, the SE type is recom-
mended for use. It is much easier to place, is more rugged, and
produces a cleaner dynamic signal than the W type. Additionally,
connector "noise" is eliminated in the SE gage because of the

47

special cable feedthrough (a significant advantage in high shock
environments). Since there is no commercially available gage which
meets the overall requirements, the SE gage design is recommended
for general use in soil stress measurements.

When placed on the surface of a soil, the gages have proven
capable of accurate measurement of pressures up to 2,000 psi; at
depths of burial greater than two gage diameters, they have accu-
rately measured pressures up to 500 psi. Measurements with the SE
gage at burial depths less than one gage diameter (2 inches) are
not recommended.

Where a minimum number of gages are to be used in sand, a
dense tamping-in placement (Method I) is recommended for general
usage. An average overregistration of about 25 percent can be ex-
pected with the dense placement method for both static and dynamic
testing at pressure levels above 150 psi.

For testing in clay, the cut/no-cover method (Method C-I),
in which the gage is placed in a matched cavity flush with the clay
surface, is recommended. The gages can be expected to underregister
by about 8 percent when statically loaded in this condition, and
overregister by 3 to 4 percent when dynamically loaded.

Difficult handling and placement problems exist in field
operations. Controlled laboratory-like environments are almost
never encountered in the field, and remote placement to some depth

is normally required, usually via drill holes. Orientation, alignment, and coupling are problems. A prepackaged gage could facilitate field handling and enhance placement uniformity. Packaging materials could be plugs of native material or artificial materials. Investigation of field placement concepts as well as borehole interaction effects is highly recommended. A laboratory study of these problems is currently underway.

APPENDIX A

DETAILS OF LABORATORY TESTS IN SOIL AND FIELD TEST RESULTS

A.1 PURPOSE AND SCOPE

The purpose of the laboratory soil tests was to determine
qualitatively, and to an extent quantitatively, the gages' reaction
to static and dynamic loads within two soil extremes: dense, dry
sand and fat, wet clay (these materials are described in detail in
Appendix B). The test program was designed to include enough
gages at a given position for statistical confidence in the
measurements.

Two rather limited field tests of the gages were conducted to
determine their performance under field conditions.

A.2 LABORATORY TEST CONDITIONS AND PROCEDURES

A.2.1 SBLG Tests. The first tests in the SBLG were conducted
with the infinite base. At the time of these tests, no effective
method for relieving chamber sidewall friction was available.
Therefore, stress losses due to wall friction at depth appear in
the initial test data. In all subsequent testing in the SBLG, a
friction-relieving membrane consisting of a sandwich of grease on
neoprene rubber was employed. The greased liner friction-relief
mechanism was developed as described in Reference 17. The use of
this liner has been found to transmit approximately 95 percent of

the applied surface pressure to depths greater than one chamber diameter (4 feet). Tests described in Reference 17 indicate that friction relief to depths of three chamber diameters or better is possible by use of this type liner.

An outline of the testing program in the SBLG follows:

Laboratory Test Program

    A. UNLINED CHAMBER TESTS[1](U)

        1. San (W and SE gages)

            a. Static--Placement Method I[2]

            b. Dynamic--Placement Method I

    B. LINED CHAMBER TESTS[1](L)

---

[1] In the unlined chamber tests, no sidewall friction relief mechanism was used. In the lined chamber tests, sidewall friction-relief liner was installed in test chamber.

[2] The placement methods are described in detail in Appendix B. For convenience, they are briefly identified as follows:

    Sand: I, tamping-in method

            II, raised-mound method

            III, set-on-surface method

    Clay: C-I, cut/no-cover method

            C-II, cut-and-cover method

            C-III, deep cut-and-backfill method

1. Sand (SE gages)

    a. Static--Placement Methods I, II, and III

    b. Dynamic--Placement Methods I, II, and III

2. Clay (SE gages)

    a. Static--Placement Methods C-I, C-II, and C-III

    b. Dynamic--Placement Methods C-I, C-II, and C-III

Unlined Chamber Tests. The initial test utilized two W
gages and two SE gages placed near the center of the test chamber
on a 9-inch radius (Figure A.1) with 12 feet of dense, dry Cook's
Bayou sand (see Appendix B) underneath. Five depths of gage cover
were evaluated: 2, 4, 6, 12, and 16 inches. The sand cover was
systematically built up by sprinkling. The gages were placed only
once, and were tamped into the soil (Placement Method I, Appendix B).
The gage array was first covered with 2 inches of sand and statically
loaded in increments to 500 psi for six cycles. Two nominal 250-psi
dynamic shots were made following the static tests. Then sand was
added until the next desired cover depth was reached and the test
sequence was repeated. This procedure was followed until all
desired depths of cover were tested. This test condition using the
dense tamping-in gage placement method and an unlined test chamber
was designated I(U).

Sand Tests in Lined Chamber. The first series of lined
chamber tests was conducted in the concrete base SBLC using dense,

dry sand (Reid-Bedford model sand; see Appendix B) and 13 SE gages placed in a geometric array at depths from 2 to 18 inches. Figure A.2 shows the gage locations and test geometry. A water bag was employed at the base of the soil column to facilitate measurement of the average transmitted pressure. Bourdon-type mechanical gages were used to measure input and transmitted pressures for the static tests, whereas Norwood gages were used for the dynamic tests. The pressure values used for the applied pressure were averaged from the input and bottom (transmitted) pressures for the static case. Only surface input pressures were used for the dynamic tests.

Three gage placement conditions were studied in this test series. Condition I(L) was a dense gage placement in which the gage was hand-tamped into the soil. Condition II(L) was a dense gage placement in which the gage was placed in an excavation in the soil, covered, and tamped (referred to as the raised-mound method). Condition III(L) was a loose placement in which the gage was simply placed on the soil surface and the remaining cover sprinkled on (set-on-surface method). Details of the placement techniques are given in Appendix B.

The test specimen was statically loaded in increments to 300 psi for six cycles. A nominal 150-psi dynamic test was made upon completion of the sixth cycle. The test specimen was then rebuilt and the gages were replaced using the next technique, and

53

the test sequence was repeated. The static data reported were taken from the first (virgin) and sixth loading cycles.

   Clay Tests in Lined Chamber. Gage placement techniques were investigated for clay as well as for sand. The same chamber, liner, and water bag base were used in this study as in the sand tests first described; however, only two depths of cover were evaluated. It was planned to test at 12- and 18-inch depths, but because of compaction, settlement, and difficulty of clay placement, the actual levels attained were 10.5 and 16.5 inches. Seven SE gages were placed at the 10.5-inch level as shown in Figure A.2b (12-inch depth). Two other gages were placed at 16.5 inches as shown in Figure A.2b (18-inch depth). Three gage placement methods were studied, as follows: Method C-I, cut/no-cover; Method C-II, cut-and-cover; Method C-III, deep cut-and-backfill.

   A.2.2 Cold Gas Loader Tests. Numerous measurements were made on the surface of a sand specimen, using an array of 4 flush-mounted SE gages, during proof tests of a new 1,000 psi-compressed (cold) gas loader. Figure A.3 is a sketch of the test chamber and gage array. Tests were made at various pressure levels up to 2,300 psi on virgin samples.

A.3 RESULTS OF TESTS IN SBLG

   A.3.1 Static Tests in Sand. Table A.1 lists the static

54

registration ratios from the unlined chamber tests for the depths tested at applied static pressures of 50, 150, 300, and 500 psi. These data are plotted in Figure A.4.

The registration ratio, or simply registration, is defined as the ratio of the stress gage output in pounds per square inch to the pressure applied to the surface of the soil specimen (or the average specimen pressure if the bottom pressure is known).

The effect of sidewall friction on the stress field is quite apparent in the plots of Figure A.4. At the high loading levels the test data closely follow the slope of the theoretical attenuation curve which was calculated from the equation (from Reference 18):

$$\frac{P_1}{P_{so}} = e^{-4\upsilon K(Z/D)}$$

where P_1 = Pressure at depth of interest

P_{so} = Pressure at the surface

υ = Coefficient of friction between medium and chamber, tan α

K = Ratio of horizontal to vertical pressure over the total cross-sectional area

Z = Depth of interest

D = Inside diameter of chamber

α = Angle of friction between medium and chamber

The assumptions made for these calculations were the use of a steel

55

chaml i, a dense, dry sand having a friction angle of about 30 degrees, a K factor of 35, with the resultant $v = 0.57$.

The gage registrations and scatter limits were noticeably large at the lower pressure loadings, but progressively decreased with increasing load for both gage types. The SE gage registrations ranged from about 1.5 (as taken from the deviation of the slope from the sidewall friction curve) at 50-psi loading to about 1.1 at 500-psi loading. The W gage values for the same range varied from about 1.45 to about 1.2.

Figure A.5 shows the SE and W gage average static registrations as a function of applied pressure for the various depths tested.

Static registrations in the lined chamber are listed (Table A.2) for loadings of 50, 150, and 300 psi. Figure A.6 presents plots of average static registrations with depth of burial for the various placement conditions in both virgin and preloaded (6th cycle) specimens. It can be seen from these data that gage registrations for all placement conditions except III(L) decreased with increasing load as they did in Test I(U). The densest placement condition, I(L), produced the highest average registrations for all depths and loadings (about 1.3 at 50 psi to 1.2 at 300 psi), while the loose placement condition, III(L), produced the lowest average registrations (the average data showing essentially no overregistration). Condition II(L) data were intermediate. Scatter was consistently

lower for Test I(L), progressing to II(L), which had the highest
scatter. Figure A.7 shows plots of average static registrations as
a function of depth of burial and applied pressure. Test III(L)
data (Figure A.7c) show the tightest grouping and best overall
linearity of the average data. However, the data scatter, which
is not shown, is significant for this burial condition. Little
change in average registration was noted from virgin loadings to
the preloaded tests (6th cycle) for the loose gage placement
(III(L)), progressing to considerable change for the raised-mound
placement (II(L)). The data scatter improved greatly with repeti-
tive loading for all gage placement conditions.

A.3.2 Dynamic Tests in Sand.

Curve-Averaging Technique. Typical SE and W gage dynamic
signatures at various depths of burial in the unlined chamber are
shown in Figure A.8. Dynamic gage registration is plotted in
Figure A.9. The pronounced damped oscillation appearing in the
early gage signal is a wave "reflection" or interaction phenomenon
which is characteristic of the SBLG test devices. Precise regis-
tration values cannot be derived from actual signatures at early
times (less than 10 msec) in sand tests because the initial stress
wave input is masked in this time frame by a "reflected" wave
occurring within the device. The bonnet (or surface input) dynamic
gas pressure remains relatively constant throughout this period, but

57

as can be seen in Figure A.10 the water bag base is subjected to a high shock level several times the magnitude of the input stress. This wave can be seen propagating back up the specimen as in Figure A.12. In light of this restriction, an average peak soil pressure was extracted from the gage waveforms by a curve-averaging technique. The oscillatory decay of the measured pressure pulse was graphically averaged and intersected with the extrapolated initial amplitude slope. This point of intersection was taken as the peak incident pressure (although this is not necessarily accurate with respect to time, it does provide reasonable peak amplitude). The inset in Figure A.8 shows the averaging method used.

Unlined Chamber Tests. Table A.3 lists the average peak dynamic registrations measured in the unlined chamber. Figure A.9 plots dynamic registrations versus gage depth for Shots 1 and 2, respectively. More uniformity in data was noted for the first shot than for Shot 2. This was probably due to a substantial disturbance of the soil by Shot 1. The SE gage data showed better repeatability and cleaner signals at early times (less than 5 msec) than that from the W gages. A somewhat spurious negative-going signal near initiation was noted occasionally on W gage signatures, Figure A.8. This interference is generally not seen in the SE signals and is thought to be due in part to the built-in subminiature cable connector of the W gages.

58

The SE gage registration (as measured from the sidewall friction curve) was approximately 1.13 for Shot 1 and 1.14 for Shot 2. W gage registrations were not as relatable.

The generally superior performance of the SE gages in this test series I(U) was readily apparent. The SE gage was determined to be more suitable for measurement; therefore, the W gage design was abandoned. All subsequent tests were made using only the SE gage.

Lined Chamber Tests. Dynamic stress waveforms recorded in the lined chamber are shown in Figure A.10. Dynamic gage registrations versus depth in the lined chamber are shown graphically in Figure A.11 and in tabular form, Table A.4. Tests I(L) and II(L) data exhibited a relatively constant registration (approximately 1.2 to 1.3) from the 6- to 18-inch depth. Both conditions exhibited the same curve shape. Test III(L) data produced a slightly different shape curve and indicated a registration of about 1.0 from 6 to 18 inches. Data scatter was about the same for all placement conditions.

Figure A.12 presents motion arrival times at depth for the various gage placement methods along with the seismic velocity band for the sand medium. The incident stress propagation is seen to fall generally within this band. The reflected stress wave, however, is seen to propagate much faster than the seismic velocity. This is thought to be due to the reflection occurring within the sand mass

59

while the sand was in a state of high compression. The transmission in the new regime would be higher than that in the normal density state.

A.3.3 Static Tests in Clay. Data were available from both depths for the dynamic tests, but only for the 10.5-inch depth for the static tests. Static data are presented in Table A.5. A plot of average registrations versus applied pressure for the various gage placements is shown as Figure A.13. Virgin loadings are shown as solid lines while the sixth loading is shown as a dashed line. The data grouping for the various placements became tighter with both repetitive loading and increasing pressure.

For the preloaded condition, Test C-II showed a linear decrease in registration with increasing load, ranging from an average of 1.12 at 50-psi to 1.0 at 300-psi loadings. Test C-I (cut/no-cover) showed an almost constant registration throughout the loading range at an average value of about 0.92. Test C-III curve (deep cut-and-backfill) was similar to that of Test C-I, but had a more pronounced curvature and slightly higher registrations. Scatter in the data was similar for all three test conditions.

A.3.4 Dynamic Tests in Clay. The dynamic data are shown in Table A.6. Typical SE gage dynamic signatures in clay are shown as Figure A.14. Tests C-I and C-III had parallel responses with negative slopes from the 10.5- to 16.5-inch depth. Test C-II had a

60

positive slope for the same region. Scatter was least for Test
C-III, increasing to Test C-II. Test C-I showed minimum registra-
tion (about 1.03 at 10.5 inches), while Test C-II showed maximum
registration (about 1.32 at 10.5 inches).

The stress transmission, a function of gage-media coupling,
was best for condition C-I, as shown by Figure A.15. The first
motion arrival times were somewhat slower than the seismic velocity
for the clay, showing a velocity increase near the base of the
specimen. Propagation of the reflected stress from the base of the
chamber is seen to be significantly faster than seismic velocity.
As in the case of the sand tests, this increased propagation veloc-
ity is probably due to the reflection occurring within the clay mass
while the clay was in a state of high compression.

Analysis of the data, both static and dynamic, leads to the
conclusion that Method C-I is the best method of SE gage placement
for testing in clay.

A.4 RESULTS OF COLD GAS LOADER TESTS

Results of the gas loader tests point out the SE gage's
ability to faithfully record dynamic surface loadings on a granular
medium. The consistency of the measurements and the agreement in
waveforms of the input air pressure and the surface loadings are
apparent in Figure A.16. The average pressure measured by the

61

flush-mounted SE gages was 10 percent higher than was measured with the reference (air pressure) gage in the fluid chamber for the 1,000-psi load. The SE gages and air pressure gage produced essentially equal measurements in the 2,300-psi loading.

A.5   FIELD TESTS

A.5.1 Operation Snowball. Four developmental gages (two W and two SE) were used to monitor earth stresses in the 1964 Canadian Project Snowball experiment conducted at the Suffield Experimental Station (SES) near Ralston, Alberta, Canada. The explosion was generated by a 500-ton hemisphere of TNT placed at ground level. The gages were placed in a vertical array (in a common hole) at the predicted 310-psi airblast location. A detailed description of the test geometry, geology, and results of ground motion measurements is given in Reference 1.

Peak stresses were predicted using the method of Newmark (Reference 19) with modifications by Hendron.[3] Figure A.17a shows pressure-time records from the four gages buried at depths of 0.5, 2.0, 8.0, and 12.2 feet; Figure A17b compares measured peak pressure values to predictions (after Hendron) and two stress values

---

[3] A. J. Hendron; verbal communications, 1964; U. S. Army Engineer Waterways Experiment Station, CE, Vicksburg, Miss.

calculated from independent particle velocity measurements. Generally, the wave shapes of the stress-time records are what would be expected, i.e., amplitude attenuation and increased rise time with depth. However, the shallowest gage (0.5-foot-deep) recorded two distinct peaks of much higher amplitude than predicted. Although no explanation of the amplitude disparity is offered (other than a possible calibration error), it is suggested that the first sharp pressure peak could possibly have been the precursor (dubbed "Roadrunner Wave") which was observed in some of the SES shock photographs by Dewey (Reference 20). An argument in support of this hypothesis is the close agreement in arrival times of the airblast at this distance (measured by Ballistic Research Laboratories[4]) and the arrival of the second peak at the 0.5-foot-deep soil stress gage.

In addition to the above, the arrival time at the 12.2-foot depth was some 9 msec late when compared to an adjacent accelerometer and an extrapolation from the other stress gages. There is a possibility (which cannot be resolved) that recording channels

---

[4] U. S. Army Ballistic Research Laboratories, Aberdeen Proving Ground, Maryland; Letter to: U. S. Army Engineer Waterways Experiment Station, Vicksburg, Miss.; Subject: Transmittal of Snowball Data, 17 November 1964.

might have become erroneously exchanged and that the measurements at the 12.2-foot-deep stress station is in reality a particle velocity measurement (of unknown scale factor) at another location.

In spite of these difficulties, the stress gages appeared to perform rather well on the whole. Response was adequate, placement was effective, and overall results indicated that the gages were suitable for field measurements.

A.5.2 Loess Tests. A limited test was conducted in 1965 in a silty loess deposit. Two-pound spherical charges of TNT explosive were used to determine coupling efficiency of small buried charges.[5] In order to alleviate nuisance problems with noise, airblast, and ejecta, the tests were conducted in the side of a covered trench. The vertical cut represented the ground surface. The HE charges were fired first at the ground surface $(\lambda_D = 0)$, then at deeper containment $(\lambda_D = 1/4, 1/2, 3/4, \text{ and } 1)$ where essentially all of the energy goes into the ground. λ is a scaled distance obtained by taking the cube root of the charge weight (in pounds). In this case, λ (feet) $= \sqrt[3]{2 \text{ (pounds)}} = 1.26$ feet. Particle velocity gages were placed in the ground on a line normal to the surface beneath the charge to sense radial velocity. A limited number of particle

_____

[5] J. K. Ingram; 1965; Unpublished data.

acceleration and soil stress gages were included for correlation with the primary velocity data. A schematic of the test array is shown as Figure A.18a.

The stress gages produced good data, showing the stress pulse modification with distance from the explosive charge, as can be seen in Figure A.18b. Stresses calculated from particle velocity data compared favorably with the measured values. A typical comparison is shown in the stress-distance plot of Figure A.19.

TABLE A.1 STATIC REGISTRATION, SBLG SAND TEST I(U)

Gage Depth	No. Data Points	Gage Type	Static Registration Ratio (Mean Values) = Measured Stress / Applied Stress							
			50 psi	Limits	150 psi	Limits	300 psi	Limits	500 psi	Limits
inch										
0	2	SE	1.30	1.06-1.54	1.13	1.00-1.31	1.13	0.99-1.22	1.05	0.98-1.14
	2	W	1.12	1.00-1.24	1.13	0.98-1.28	1.14	0.97-1.30	0.99	0.96-1.02
2	2	SE	1.29	1.18-1.40	1.24	1.14-1.34	1.18	1.10-1.27	1.11	1.05-1.18
	2	W	1.18	1.10-1.26	1.17	1.07-1.27	1.16	1.07-1.27	1.17	1.08-1.26
4	2	SE	1.48	1.16-1.80	1.29	1.12-1.46	1.16	1.07-1.26	1.07	1.02-1.11
	2	W	1.44	1.24-1.64	1.29	1.07-1.52	1.16	1.06-1.26	1.13	1.02-1.24
6	2	SE	1.40	1.20-1.60	1.23	1.13-1.34	1.14	1.07-1.21	1.07	1.02-1.11
	2	W	1.35	1.20-1.50	1.22	1.10-1.34	1.16	1.05-1.27	1.13	1.00-1.26
12	2	SE	1.08	0.98-1.18	0.99	0.94-1.05	0.95	0.90-0.99	0.91	0.88-0.94
	2	W	1.18	1.16-1.20	1.08	1.03-1.13	1.00	0.93-1.07	0.95	0.86-1.03
16	2	SE	0.92	0.84-1.00	0.90	0.82-0.98	0.86	0.81-0.90	0.84	0.79-0.88
	2	W	0.97	0.80-1.14	0.92	0.83-1.01	0.90	0.82-0.99	0.87	0.80-0.94

TABLE A.2 STATIC REGISTRATION, SPLG SAND TESTS I(L), II(L), AND III(L)

Gage Placement Condition	Depth	No. Data Points	Static Registration Ratio (Mean Values)				Measured Stress Average Applied Stress	
			50 psi	Limits	150 psi	Limits	300 psi	Limits
	inch							
Virgin Specimen:								
I(L)	2	1	1.33	--	No data	--	1.20	--
II(L)	2	2	1.02	0.91-1.14	1.03	0.97-1.08	0.92	0.96-1.06
III(L)	2	2	0.84	0.39-1.29	0.94	0.44-1.23	0.94	0.73-1.16
I(L)	6	2	1.46	1.40-1.52	1.32	1.31-1.36	1.29	1.20-1.30
II(L)	6	2	1.57	1.37-1.76	1.45	1.26-1.64	1.35	1.14-1.52
III(L)	5	2	0.91	0.77-1.05	0.91	0.82-1.00	0.92	0.85-0.97
I(L)	12	7	1.45	1.26-1.64	1.36	1.16-1.79	1.29	1.14-1.40
II(L)	12	6	1.40	1.11-1.82	1.34	1.08-1.73	1.30	1.01-1.63
III(L)	12	7	1.06	0.75-1.38	1.06	0.73-1.31	1.04	0.73-1.25
I(L)	18	2	1.40	1.38-1.42	1.26	1.26-1.26	1.11	0.90-1.31
II(L)	18	No data	No data	--	No data	--	No data	--
III(L)	18	2	0.99	0.84-1.14	0.97	0.82-1.10	0.96	1.46-1.96
Preloaded Specimen:								
I(L)	2	1	1.206[a]	--	1.061[a]	--	1.10[a]	--
II(L)	2	2	1.008	1.006-1.010	0.97	0.96-0.98	0.960	0.96-0.96
III(L)	2	2	1.070	0.944-1.1%	0.84	0.60-1.06	0.960	0.60-1.30
I(L)	6	2	1.433	1.394-1.475	1.309	1.30-1.32	1.34	1.14-1.54
II(L)	6	2	1.340	1.170-1.510	1.357	1.19-1.52	1.315	1.09-1.54
III(L)	6	2	0.994	0.948-1.02	0.913	0.85-0.97	0.941	0.92-0.96
I(L)	12	7	1.340	1.190-1.490	1.35	1.15-1.56	1.35	1.15-1.53
II(L)	12	7	1.338	0.730-1.949	1.155	0.935-1.40	1.111	0.94-1.25
III(L)	12	7	1.070	0.822-1.1%	1.32	0.932-1.15%	1.210	0.97-1.55
I(L)	18	2	1.393[a]	--	1.31	1.09-1.53	1.29%	1.10-1.20
II(L)	18	2	No data	No data	No data	No data	No data	No data
III(L)	18	2	0.890	1.94-2.88	1.0	1.09-1.30	1.0	1.06-1.09

[a] Single gage data.

TABLE A.3 DYNAMIC REGISTRATION, SBLG SAND TEST I(U)

$$\text{Dynamic Registration (Mean Values)} = \frac{\text{Measured Stress (Averaged Peak)}}{\text{Applied Stress (Airblast Pressure)}}$$

Gage Depth	No. Data Points	Gage Type	Shot 1			Shot 2		
			P_{so}	Registration	Limits	P_{so}	Registration	Limits
inch								
2	2	SE	285	1.06	1.00-1.12	264	1.09	1.01-1.16
	2	W	285	0.75	0.72-0.80	264	1.17	1.10-1.24
4	2	SE	263	1.07	1.01-1.13	244	1.20	1.15-1.25
	2	W	263	0.82	0.80-0.83	244	1.05	1.00-1.10
6	2	SE	242	1.07	0.99-1.06	223	1.06	1.00-1.12
	2	W	242	0.91	0.91-0.91	223	0.85	0.84-0.86
12	2	SE	266	0.93	0.93-0.93	250	0.95	0.88-1.02
	1	W	266	0.90	--	250	0.93	0.80-1.05
16	2	SE	267	0.84	0.80-0.88	246	0.925	0.92-0.93
	2	W	267	0.88	0.78-0.98	246	1.095	1.09-1.10

68

TABLE A.4 DYNAMIC REGISTRATION, SBLG SAND TESTS I(L), II(L), AND III(L)

Gage Placement Condition	Depth	No. Data Points	Surface Input Pressure	Average Measured Pressure	Limits	Registration	
						Average Registration	Limits
	inch		psi	psi	psi		
I(L)	2	1	150	150	--	1.00	--
	6	2	150	195	180-210	1.30	1.20-1.40
	12	7	150	187	175-201	1.25	1.17-1.34
	18	2	150	210	210-210	1.40	1.40-1.40
II(L)	2	2	150	120	100-140	0.80	0.67-0.93
	6	2	150	183	165-200	1.22	1.10-1.33
	12	6	150	164	150-1?	1.09	1.00-1.16
	18	2	150	200	195-2??	1.34	1.30-1.37
III(L)	2	2	140	116	72-160	0.83	0.51-1.14
	6	2	140	132	120-145	0.95	0.86-1.04
	12	6	140	157	140-172	1.12	1.00-1.23
	18	2	140	135	120-140	0.96	0.93-1.00

TABLE A.5 STATIC REGISTRATION, SBLG CLAY TESTS C-I, C-II, and C-III

Gage Placement Condition	Depth	No. Data Points	Static Registration (6th Loading Cycle)					
	inch		50 psi	Limits	150 psi	Limits	300 psi	Limits
Virgin Specimen:								
C-I	10.5	6	0.83	0.65-1.04	0.94	0.77-0.99	0.92	0.78-1.06
C-II	10.5	6	1.20	0.65-1.58	1.10	0.92-1.28	1.01	0.86-1.12
C-III	10.5	7	1.00	0.67-1.49	0.98	0.74-1.21	0.96	0.79-1.09
Preloaded Specimen:								
C-I	10.5	6	0.92	0.66-1.01	0.96	0.81-1.01	0.92	0.80-1.00
C-II	10.5	6	1.12	0.90-1.36	1.05	0.90-1.17	1.00	0.85-1.09
C-III	10.5	7	0.83	0.64-1.12	1.02	0.76-1.24	0.95	0.75-1.03

TABLE A.6 DYNAMIC REGISTRATION, SBLG CLAY TESTS C-I, C-II, and C-III

Gage Placement Condition	Depth	Surface Input Pressure	No. Data Points	Average Measured Pressure	Limits	Average Registration	Registration Limits
	inch	psi		psi	psi		
C-I	10.5	140	6	144.6	120-155	1.03	0.86-1.11
	16.5	140	1	160.0	--	1.14	--
C-II	10.5	145	7	191.0	152-230	1.32	1.05-1.58
	16.5	145	1	170.0	--	1.17	--
C-III	10.5	144	7	166.5	150-180	1.16	1.04-1.25
	16.5	144	1	180.0	--	1.25	--

71
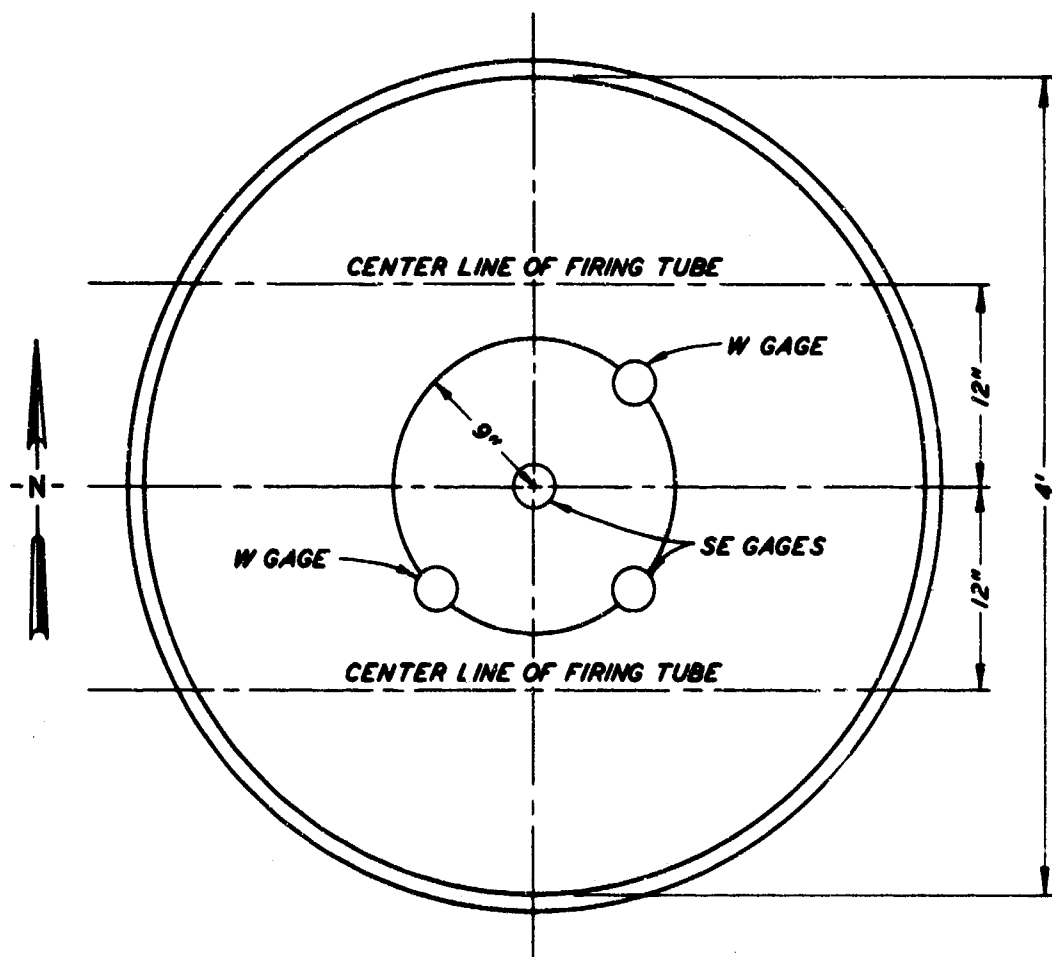
Figure A.1   Test I(U) gage placement in SBLG.

b. PLAN VIEW OF GAGE LOCATIONS

a. SECTION OF RIGID BASE SBLG
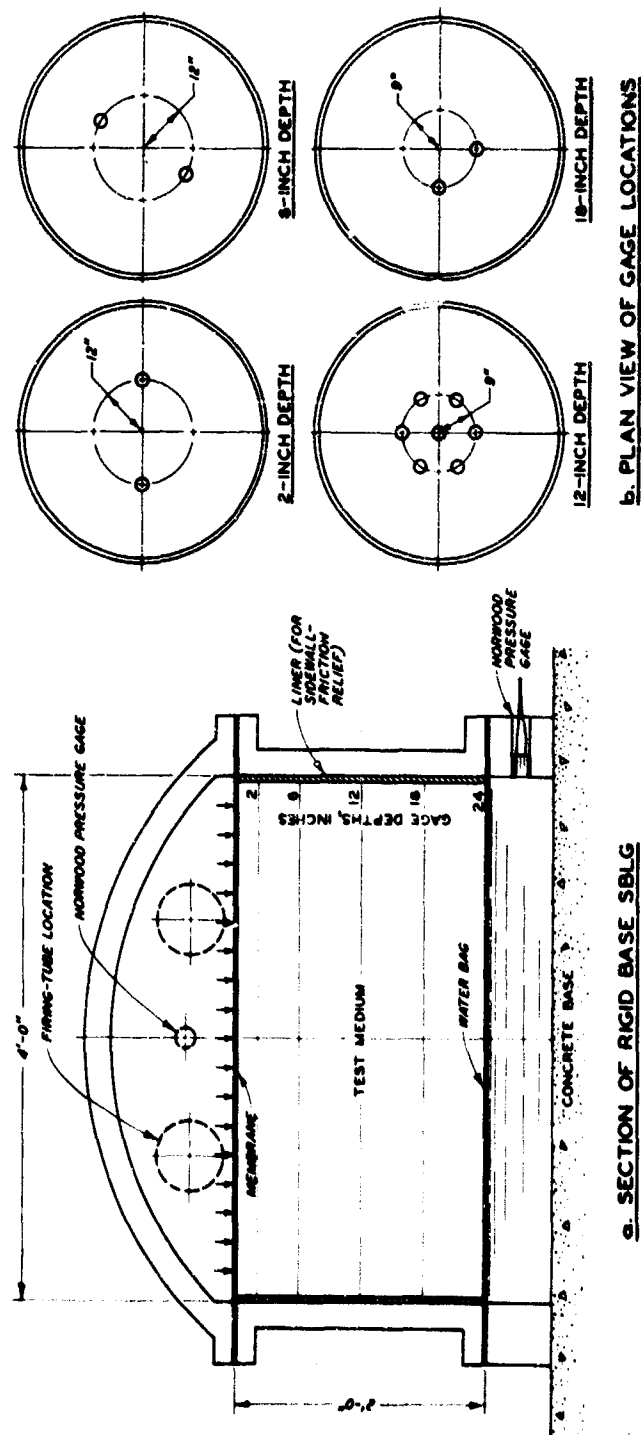
Figure A.2 Gage layout for sand test in lined SBLG.

73

PLAN

SECTION A-A
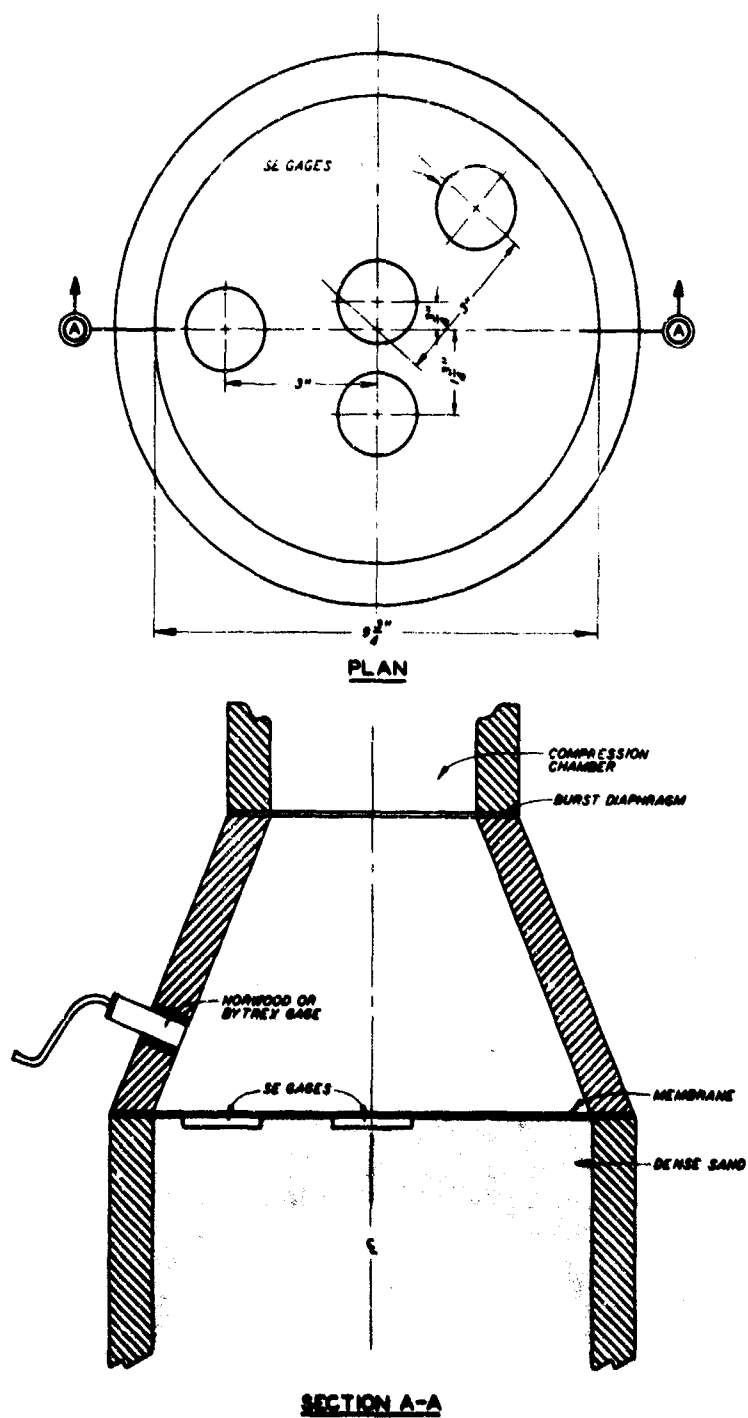
Figure A.3 Sketch of experimental cold gas loader and gages.
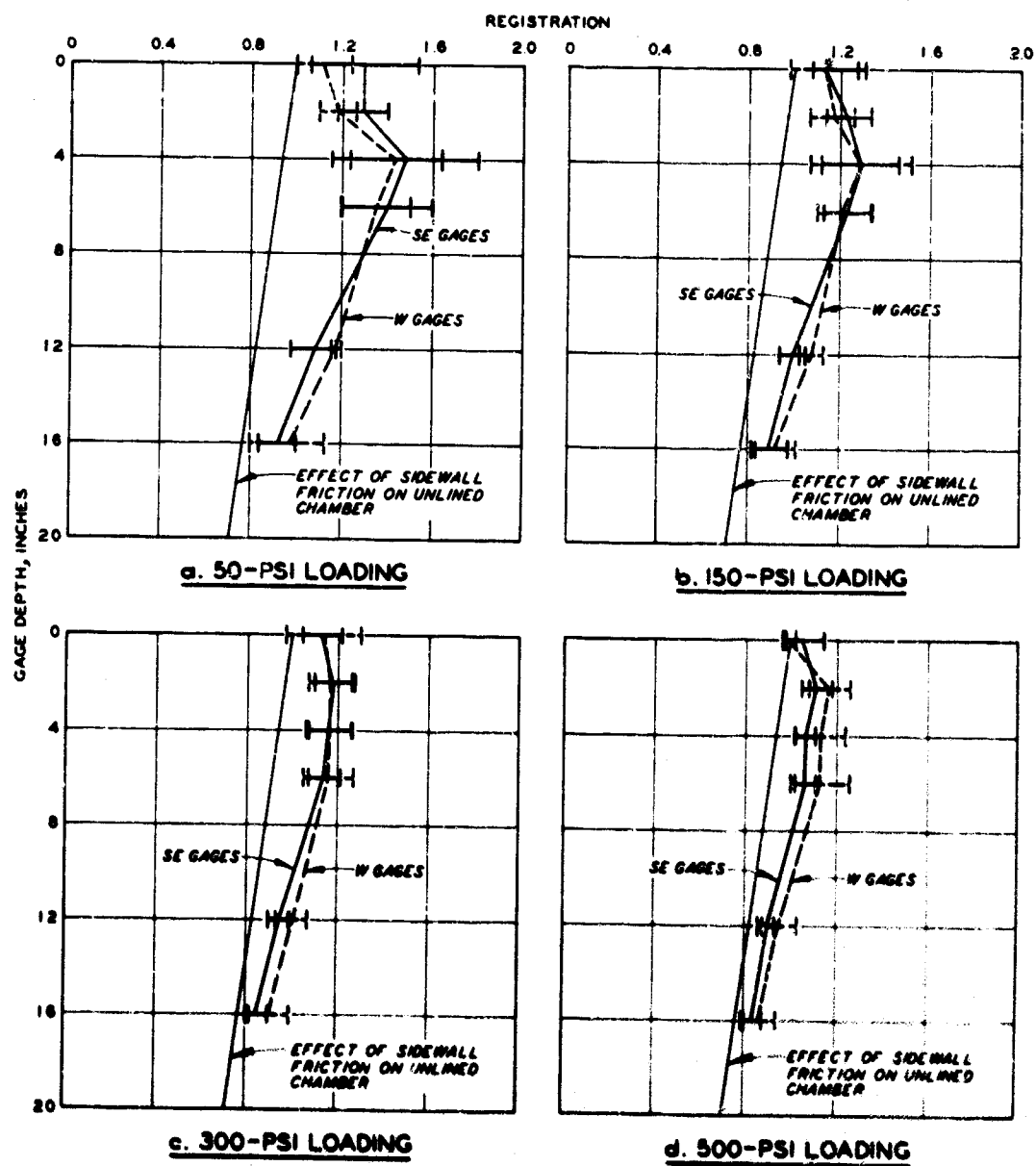
Figure A.4 Stress gages static registrations with depth, SHLG Sand Test I(U), unlined chamber.
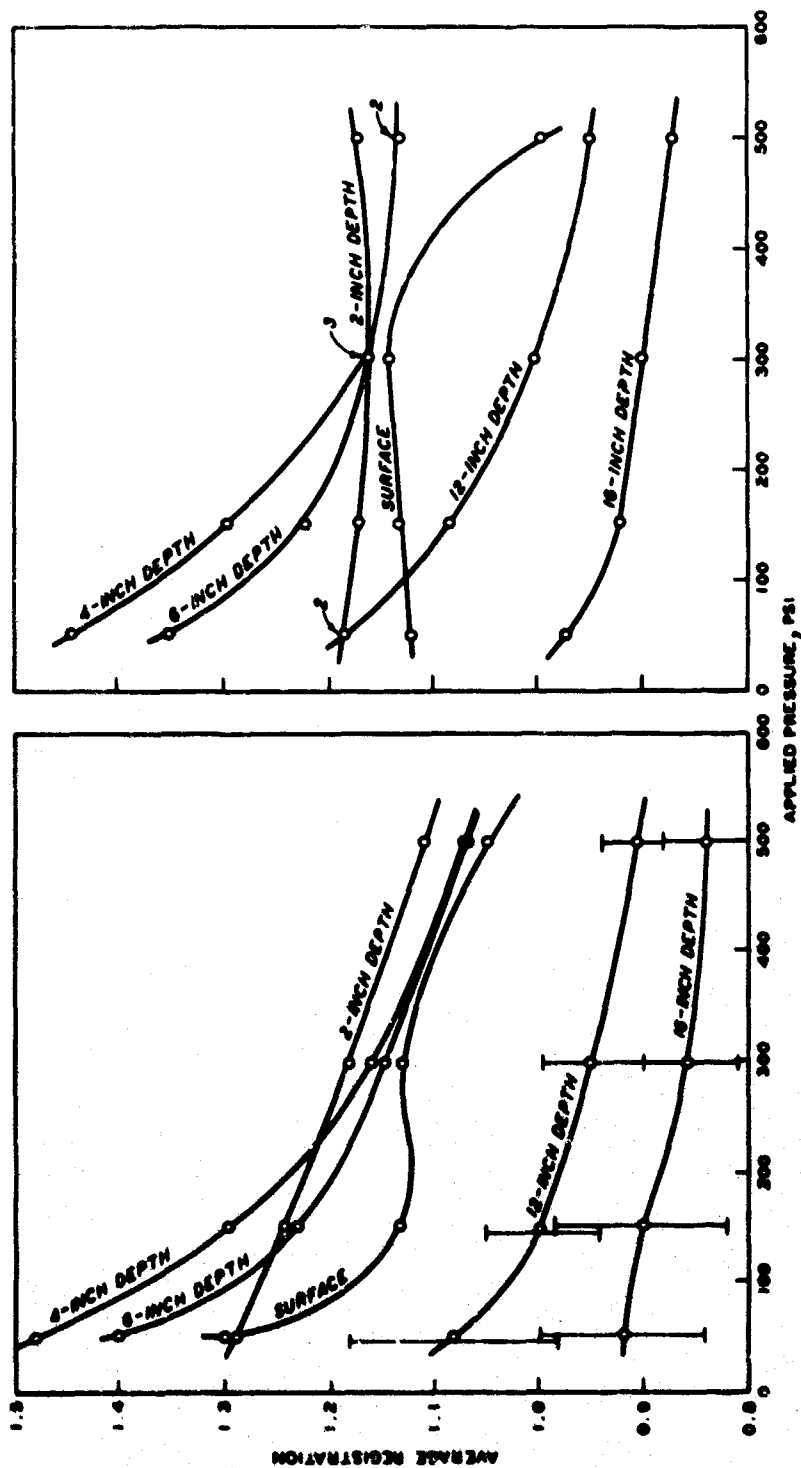
Figure A.5 Stress gages' static registration as function of depth and applied pressure in SBLG Ser Test I(U), unlined chamber.
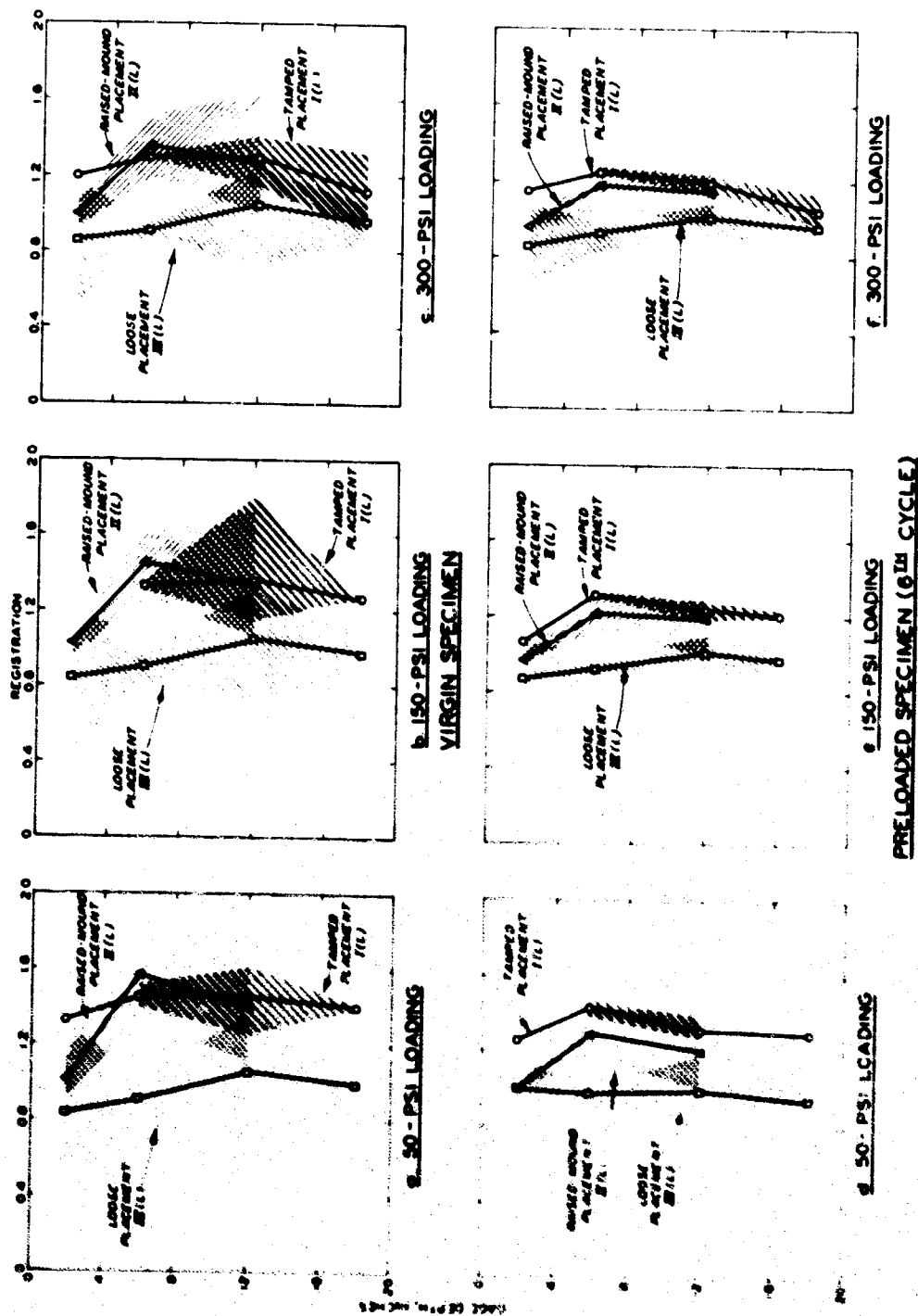
Figure A.6 SE gage static registrations in sand with 1-in. SBLG tests, lined chamber.

a. TEST I(L), TAMPED PLACEMENT   b. TEST II(L), RAISED-MOUND PLACEMENT   c. TEST III(L), LOOSE PLACEMENT
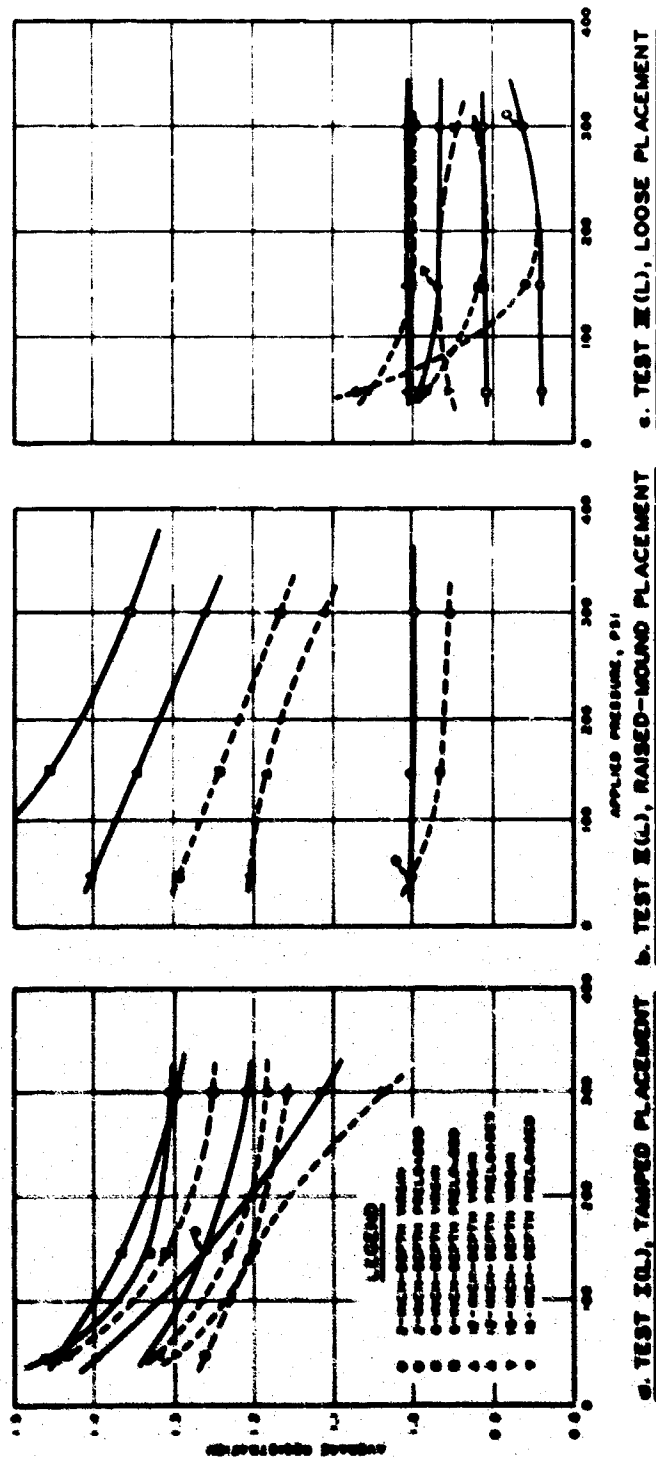
Figure A.7 SE gage static registrations as function of depth and applied pressure, SBLG sand tests, lined chamber.

78
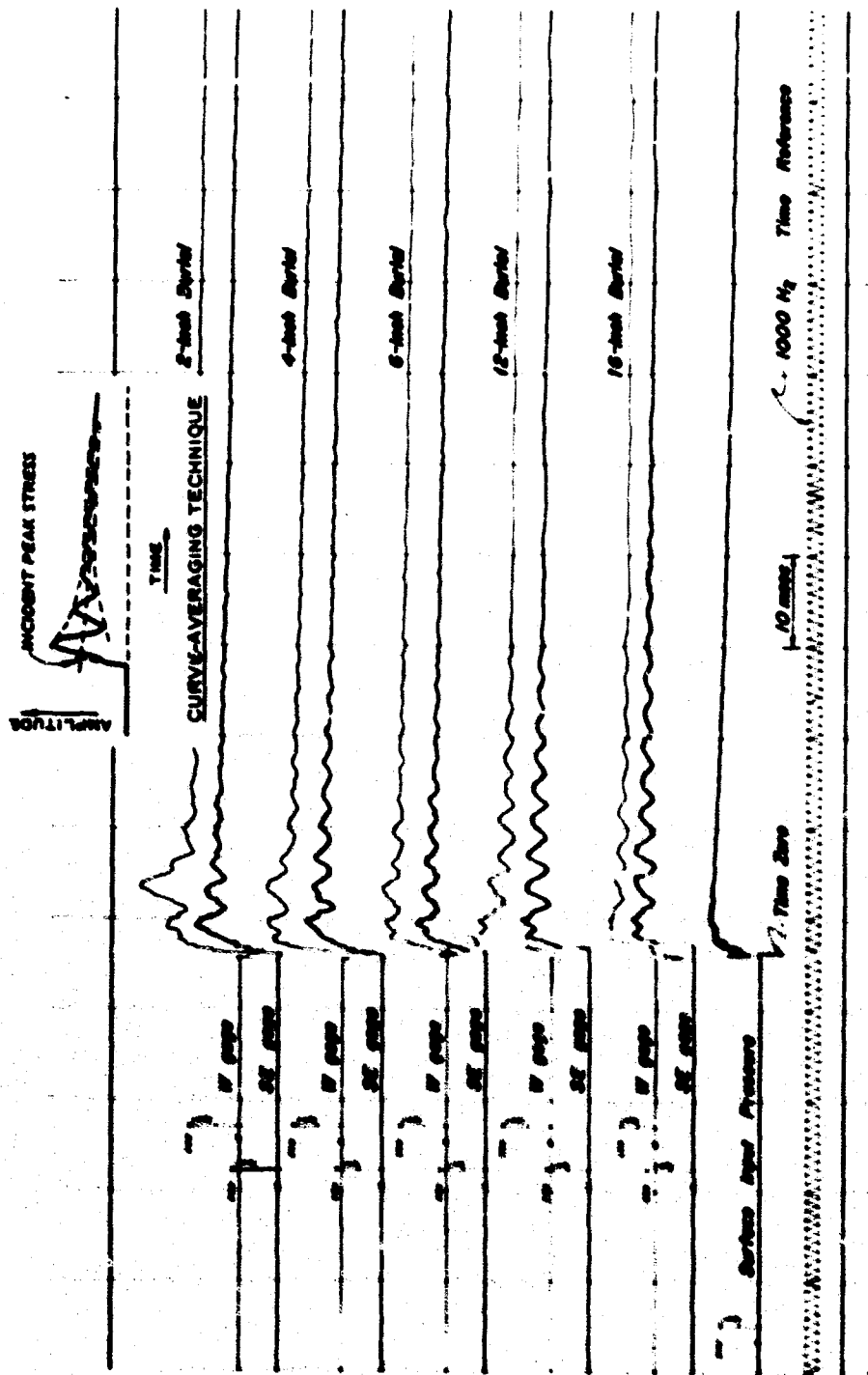
Figure A.8 Typical dynamic signatures of gages at various depths, SBLG
Sand Test I(U), unlined chamber.
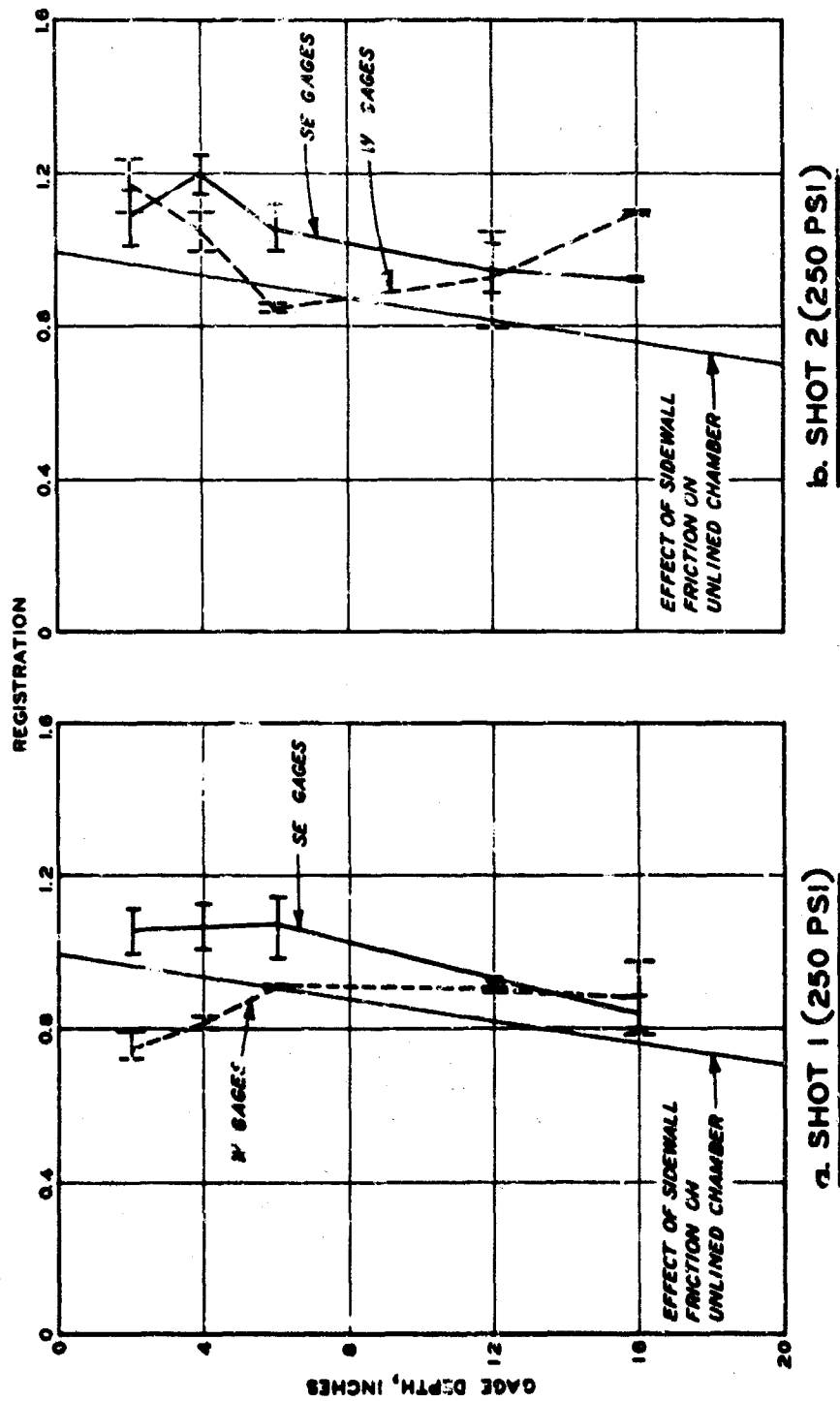
Figure A.9 Stress gages' dynamic registrations with depth, SBLG Sand Test I(U), unlined chamber.
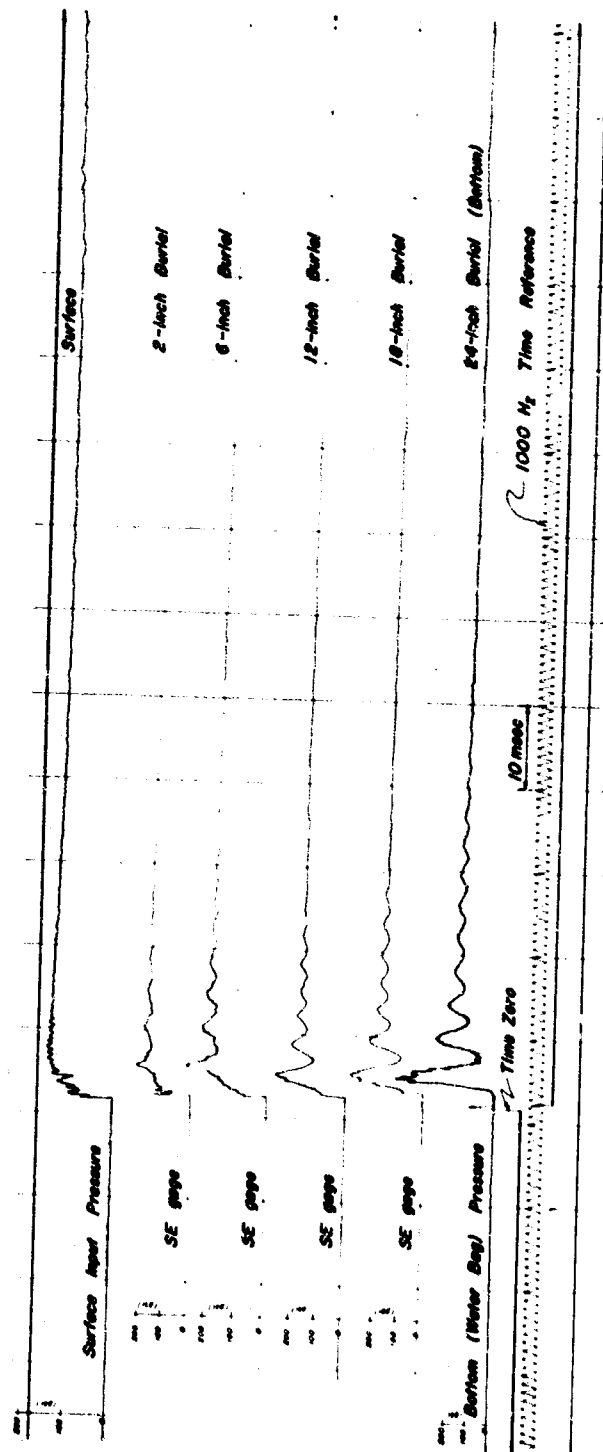
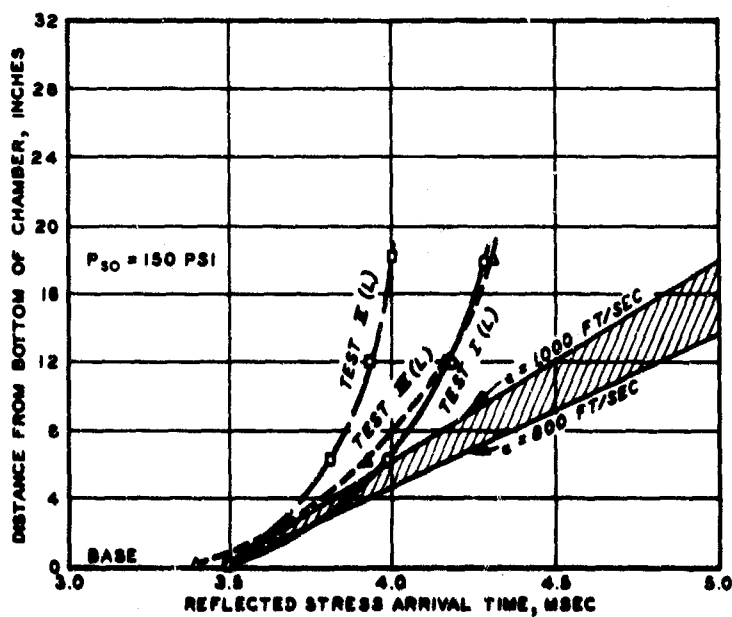Figure A.10 Typical SE gage dynamic signatures at various depths, SBLG sand tests, lined chamber.
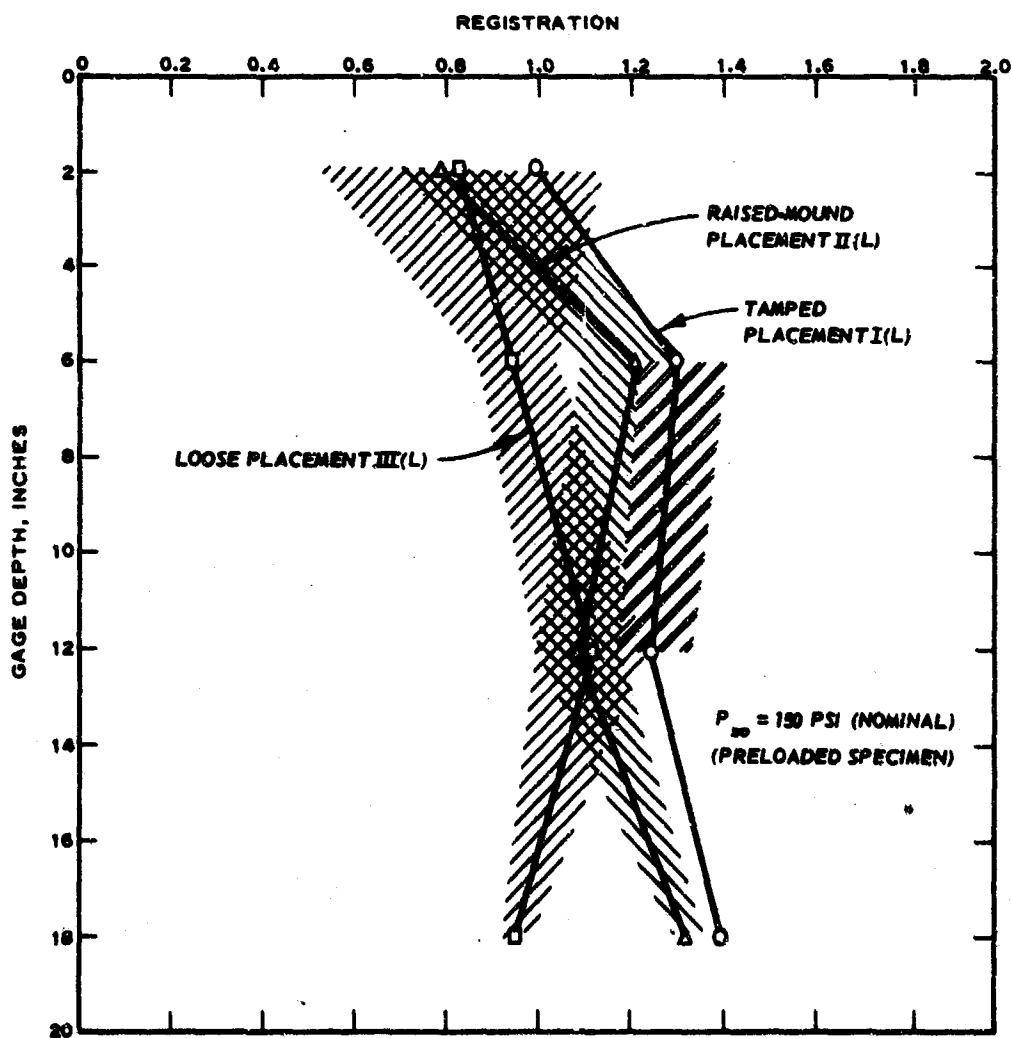
Figure A.11 SE gage dynamic registrations as function of depth
and gage placement, SBLG sand tests, lined chamber.
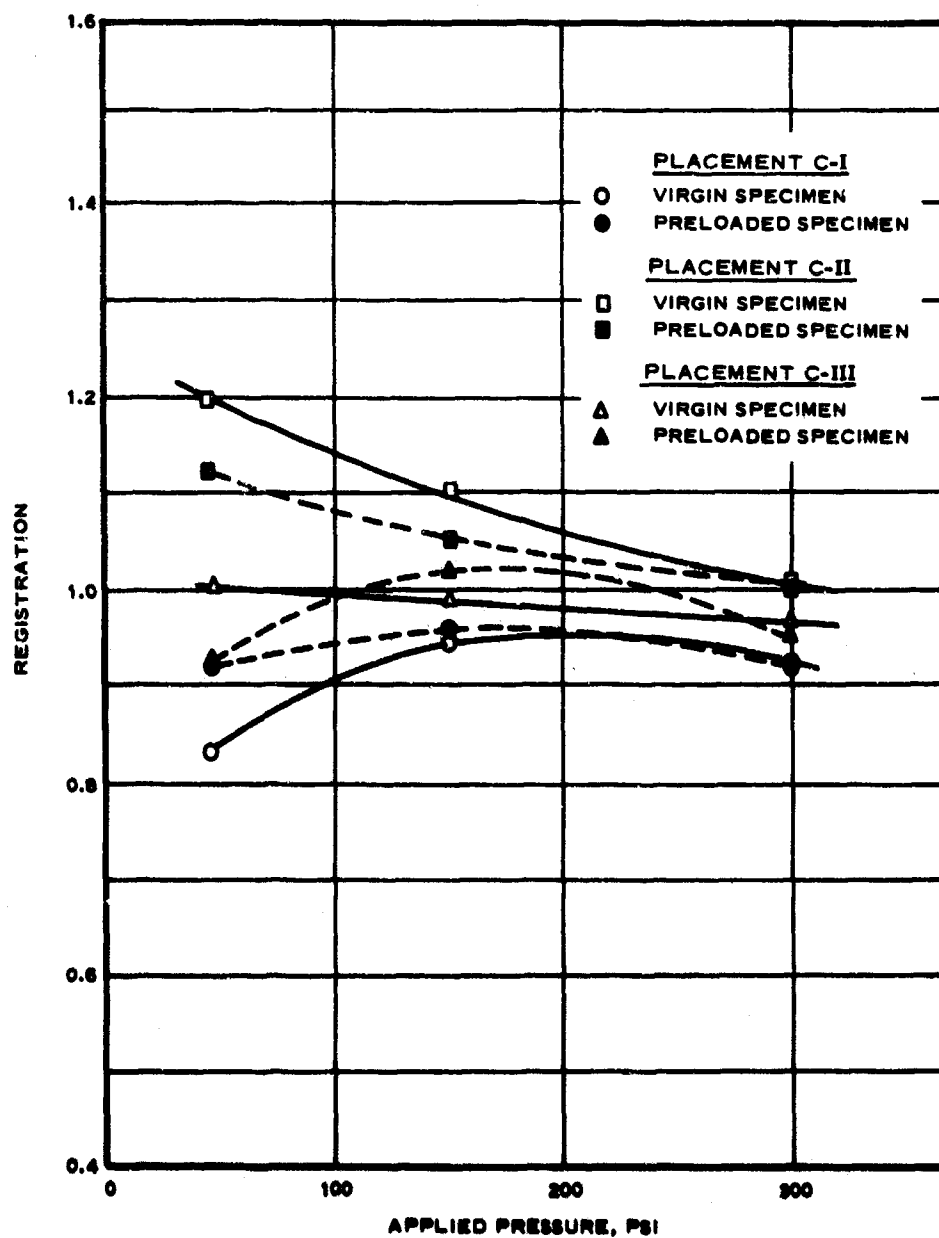
Figure A.12 Stress arrival times, SENG sand tests.

Figure A.13 Static gage registrations as a function of loading and placement, 10.5-inch depth, SBLG clay tests.
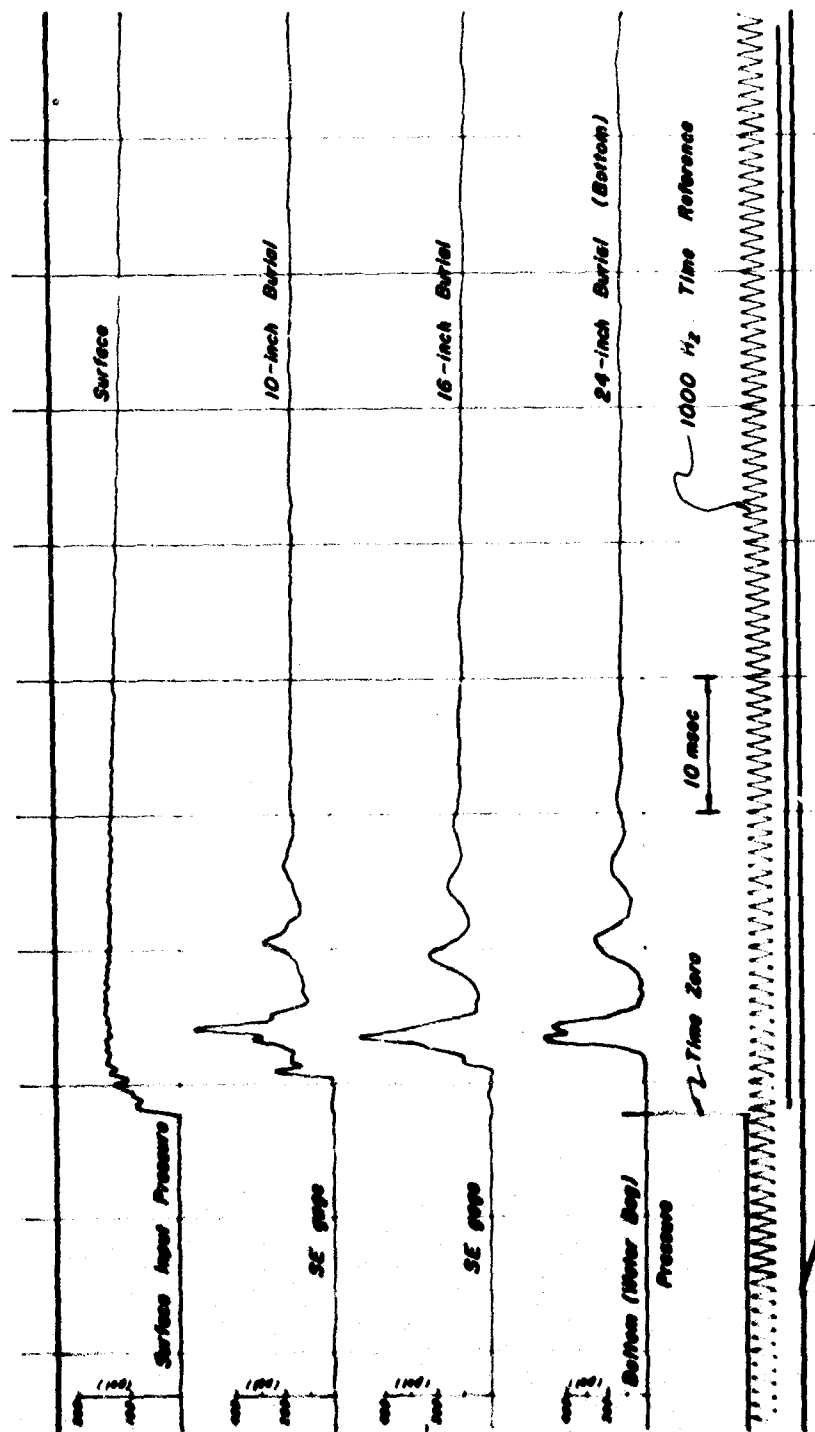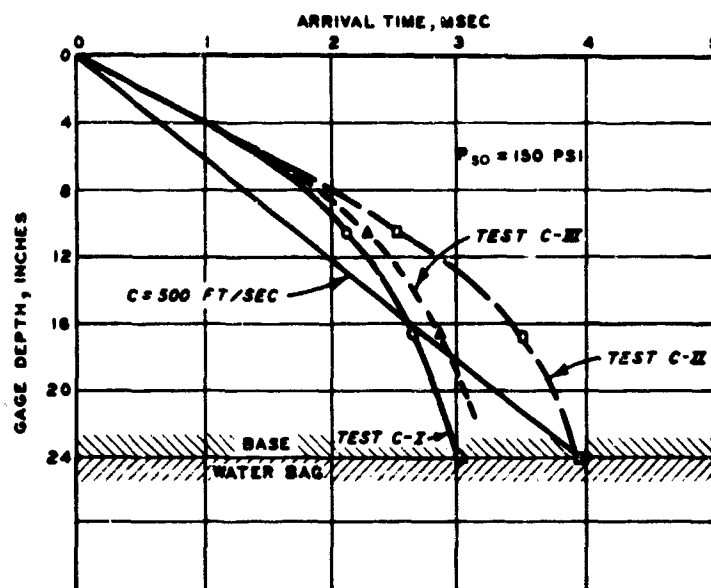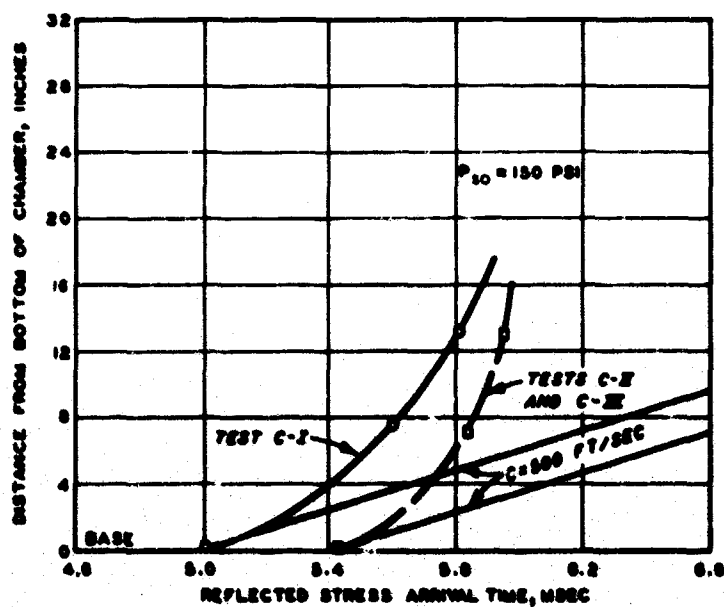
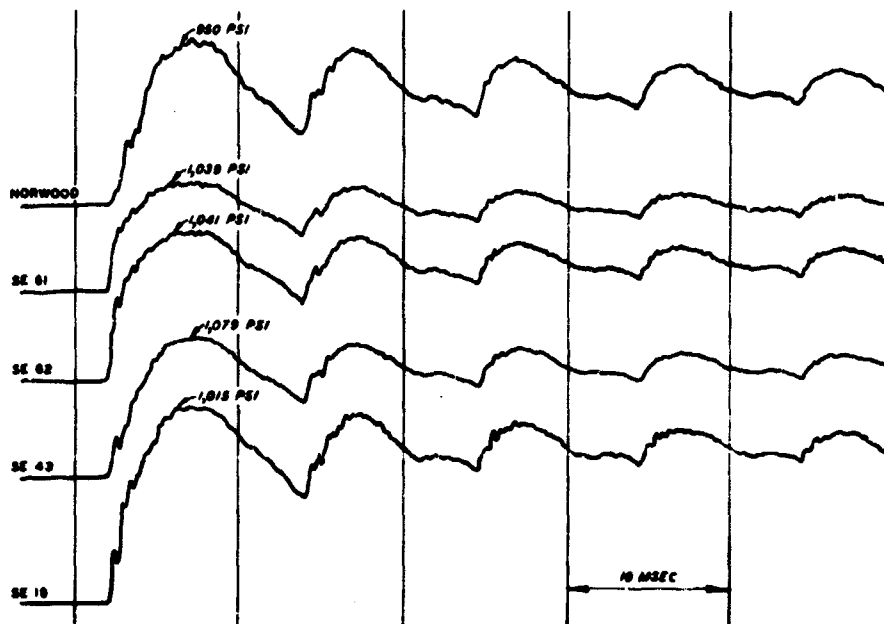Figure A.14 Typical SE gage dynamic signatures at various depths, SBLG clay tests, lined chamber.
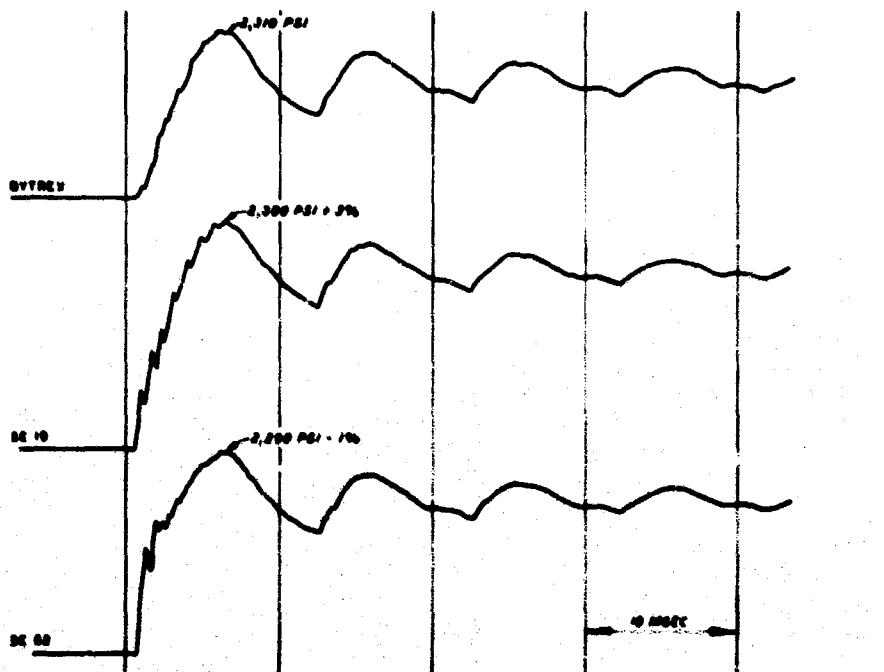
a. FIRST MOTION ARRIVAL TIME

b. REFLECTED STRESS ARRIVAL TIME

Figure A.15 Stress arrival times, SBLG clay tests.

a. NOMINAL 1,000-PSI LOADING WAVEFORM

b. NOMINAL 2,300-PSI LOADING WAVEFORM

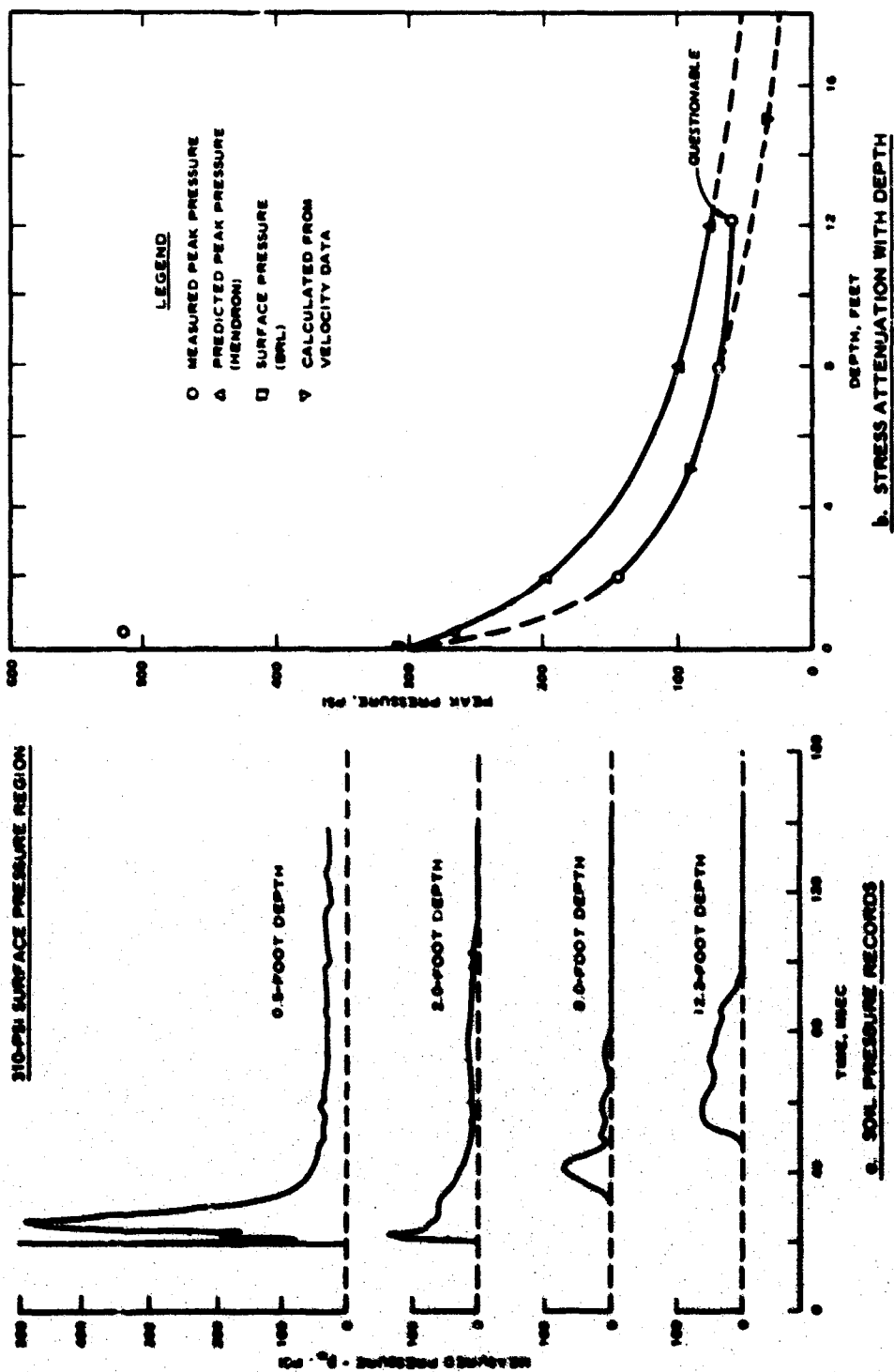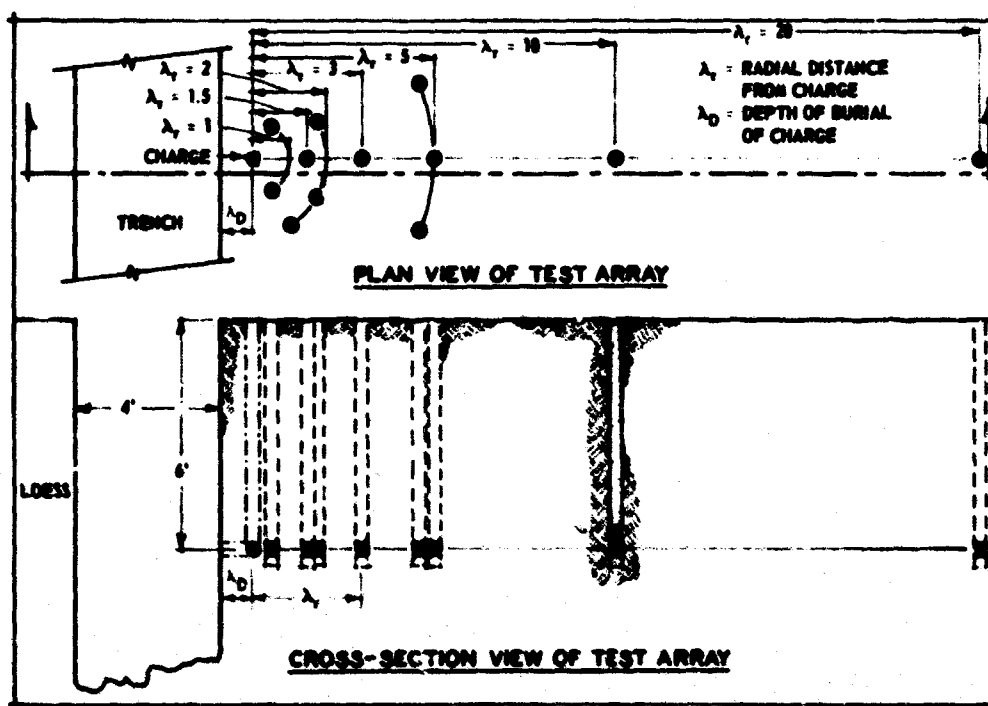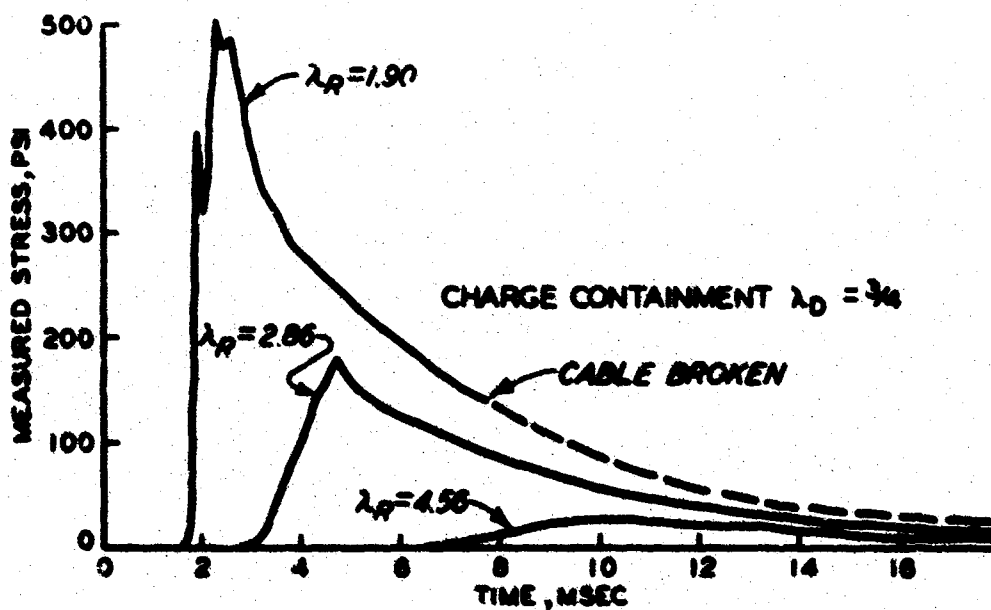Figure A.16 Typical measured waveform, cold gas loader tests.

Figure A.17 Field stress measurements, Operation Snowball.

a. Schematic of test geometry.

b. Stress waveform variance with distance from a contained charge.

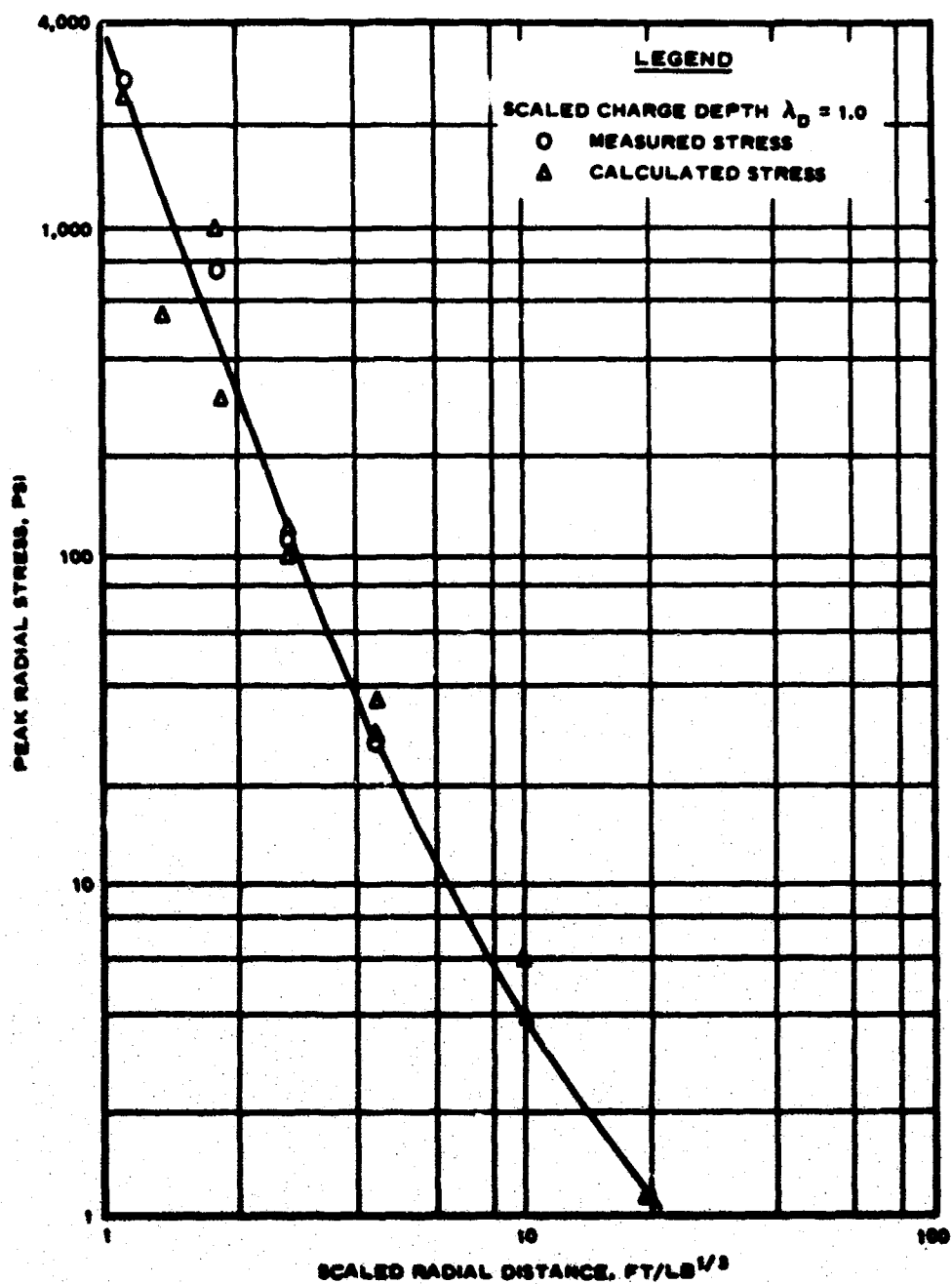Figure A.18 Loess test geometry and measured stress waveforms.

Figure A.19 Comparison of measured and computed stress as function of radial distance from charge.

90

APPENDIX B

DESCRIPTION OF TEST SOILS AND SOIL AND GAGE PLACEMENT METHODS

B.1 SAND

B.1.1 Sand Types. Two sands were used in the laboratory evaluations. Sand 1 (unlined chamber tests), known as Cook's Bayou No. 1, was a clean, uniform, medium to fine, well-graded sand, classified as SP in the Unified Soil Classification System. This sand was obtained about 7 miles northeast of the Waterways Experiment Station and is used commercially as a masonry sand. The average grain size is 0.26 mm, and the uniformity coefficient is 1.65. Individual particles vary from angular to rounded in shape with a predominance of subrounded shapes. Solids specific gravity is 2.65. This analysis was made by a standard technique.

Sand 2 (lined chamber tests), known as Reid-Bedford model sand, was also a uniform fine sand, classified as SP in the Unified Soil Classification System. The coefficient of uniformity is 1.5, and the solids specific gravity is 2.66. Predominant grain structure is subrounded to subangular.

The choice of these sands over more ideal laboratory sands, such as 20-30 Ottawa, was prompted by accessibility and by their average characteristics which more closely approach those of normal deposits.

B.1.2 Sand Placement Technique. A sand placement technique
for use in the calibration and test chambers has been developed and
adopted as standard procedure. A free sprinkling or dropping tech-
nique, originally developed by the Massachusetts Institute of Tech-
nology, was selected as the most repeatable method of deposition.
The sprinkling device itself consists of a rectangular sand bin with
12 orifices positioned in a geometrically convergent bottom, the
slopes of which are greater than the friction angle of all sands in
use, approximately 60 degrees. Metal hoses 1-1/2 feet long and
2 inches in diameter are connected to each orifice and aligned for
maximum uniformity of flow for the falling sand. Figure B.1 is a
photograph of the device in operation. The drop height and orifice
size were calibrated to give the maximum dry density attainable with
this technique, approximately 95 percent. The drop height is set at
24 inches for all sands currently in use at the laboratory. To
achieve maximum uniformity for the total sample, the device is
rotated while sprinkling the sand in the Small Blast Load Generator
(SBLG). Approximately 2 inches of sand is built up for a given drop
position (height). After this lift is completed, the sprinkler is
raised 2 inches and the sand sprinkled as before. The sequence is
repeated until the required level is achieved.

B.2 GAGE PLACEMENT TECHNIQUES IN SAND

Gage placement is a critical problem in obtaining correlative data in an in-place calibration. Experience has shown that considerable scatter in gage registrations will occur unless care is taken during gage placement. Noticeable scatter can be observed between separate placements, even with a standardized placement technique. The three gage placement techniques used in this study are discussed below.

1. Method I, tamping-in method. Sand is sprinkled in the test chamber until the gage level is reached. The gage is positioned and tamped into the sand using 40 uniform tamps of about 0.5 pounds force applied with a rubber-coated 1-inch-diameter dowel. Sand is hand-sprinkled around and over the gage, barely covering it. The area over the gage and extending approximately two gage diameters from it is then gently tamped 40 times through a thin metal plate (trowel). Sand is hand-sprinkled to cover the gage approximately 1/4 inch and the area is tamped through the metal plate an additional 40 times. The specimen is completed by sprinkling sand to the required height.

2. Method II, raised-mound method. Sand is sprinkled in the test chamber until the test level is slightly exceeded (by approximately the thickness of the gage). A volume slightly larger than that of the gage is excavated. This recessed area is tamped through

93

a thin circular metal plate 40 times. The gage is now positioned in the prepared area. Sand is hand-sprinkled to slightly cover the gage. The area over the gage and extending approximately two gage diameters from it is then gently tamped 40 times through a thin metal plate (as in Method I). An additional 1/2-inch thickness of sand is sprinkled on the gage to form a mound. The gage area is tamped 40 times through the metal plate, as previously. The specimen is completed as in Method I.

3. **Method III, Set-on-Surface Method.** The specimen is built up to the gage level and the gage positioned. Sand is then sprinkled on in the normal manner to complete the specimen.

Placement Methods I and II leave a hard spot beneath the gage, which has the effect of concentrating the stress field somewhat, thereby causing relatively high gage registration. The tests reported in Appendix A indicate that minimum mean registration could be obtained with a simple set-on-surface placement; however, this method produced more scatter and a consequently broader confidence level than did the tamping-in method. The greatest scatter of data resulted with the raised-mound method.

B.3 CLAY

The gages were laboratory-tested in a stiff local clay known as "buckshot" clay. Typical characteristics as well as placement

94

techniques are discussed in Reference 21.

B.4 GAGE PLACEMENT TECHNIQUES IN CLAY

Clay was placed in the test chamber and compacted with a
Harvard pneumatic hammer compactor with 40-pound spring. The
specimen level was brought up to the desired height and gage posi-
tion marked on the surface of the specimen. From this point the
following three methods of gage placement were used:

1. Method C-I, cut/no-cover method. A plug of clay the size
of the gage is removed with a sampler (Figure B.2a). A shallow,
tapered trench is then dug for the gage cable and the gage emplaced
(Figure B.2b). Clay is added to the specimen and compacted to
complete the required height.

2. Method C-II, cut-and-cover method. The gage is placed as
in Method C-I, but before completing the specimen, a mound of loose
clay 3/4 inch thick and 6 inches in diameter is placed on top of the
gage. This layer is compacted with 100 tamps of a miniature Harvard
compactor (Figure B.2c) and yields a final 1/2-inch-thick cover.
The specimen is completed as in Method C-I.

3. Method C-III, deep-cut-and-backfill method. A plug of
clay is removed as in Methods C-I and C-II, but the depth of cut
extends to 1-1/4 inches (Figure B.2d). The gage is emplaced and
the hole backfilled with two 5/8-inch-thick layers of loose clay.

Each layer is compacted with 8 tamps of the miniature compactor.
The specimen is completed as in Methods C-I and C-II.
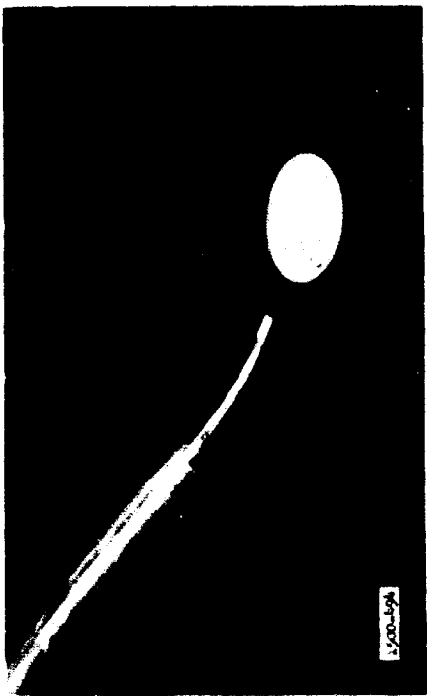
B.5 FIELD GAGE PLACEMENT

A field-gage placement device is shown schematically in Figure
B.3. This device may be used to place gages down boreholes at
depths of the order of 25 feet. The tool consists essentially of a
slotted Bakelite gage adapter attached to a hollow aluminum shaft.
Gage holding pressure is supplied to the Bakelite adapter through
two spring-steel straps. The aluminum shaft is of segmented
5-foot lengths, held together with tapered pins. This allows the
operator to lengthen or shorten the assembly to his convenience.
A truncated cone expander is attached to an aluminum guide rod
above the gage clamp. A small, lightweight aircraft cable is
attached to the other end of the rod. By pulling the cable, the
rod with expander is forced up, spreading the steel straps and the
gage adapter, thereby freeing the gage. The cable is then released
causing the adapter to close partially. The tool can now be used
to tamp the gage into the soil to ensure proper seating. After the
placement is completed, the tool is removed from the hole and the
hole backfilled with rained dry sand to the next instrument level.

96

Figure B.1 Sand sprinkling device.
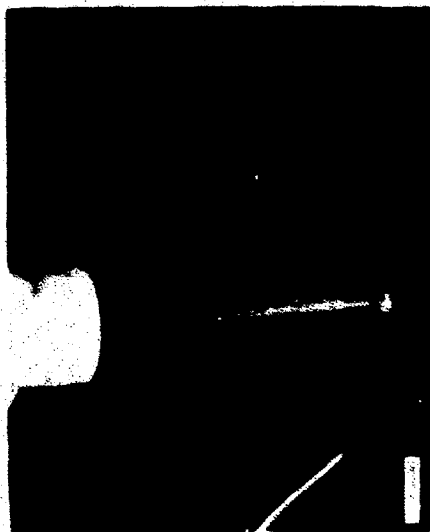
a. Clay removed for gage placement.

b. Cut/no-cover method.

c. Cut-and-cover method.

d. Deep-cut-and-backfill method.

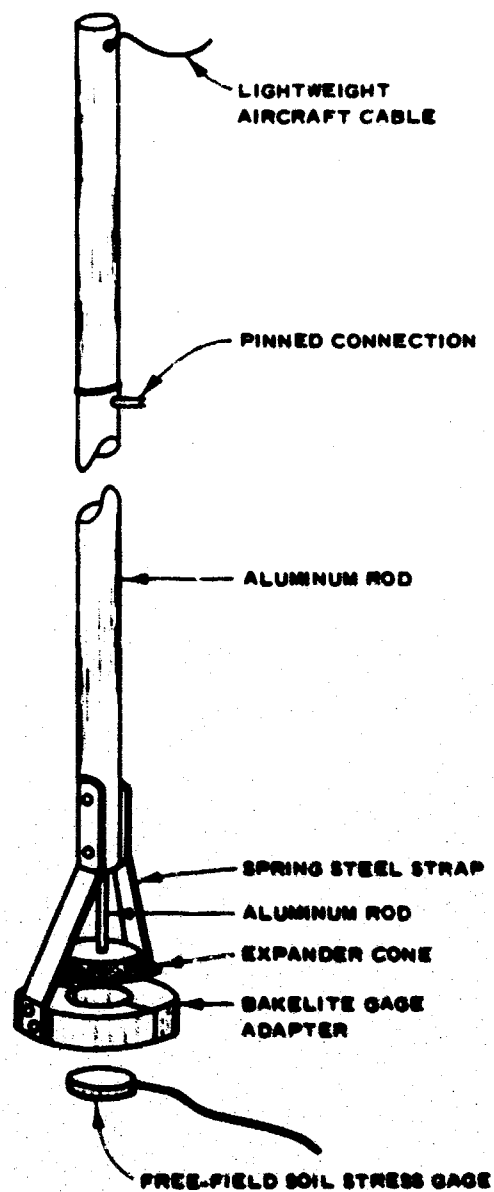Figure B.2 Methods of gage placement in clay.

Figure B.3 Gage placement device for field use.

LIGHTWEIGHT AIRCRAFT CABLE

PINNED CONNECTION

ALUMINUM ROD

SPRING STEEL STRAP

ALUMINUM ROD

EXPANDER CONE

BAKELITE GAGE ADAPTER

FREE-FIELD SOIL STRESS GAGE

99

REFERENCES

1. D. W. Murrell; "Operation Snowball, Project 3.6--Earth Motion Measurements"; Technical Report No. 1-759, March 1967; U. S. Army Engineer Waterways Experiment Station, CE, Vicksburg, Miss.; Unclassified.

2. U. S. Army Engineer Waterways Experiment Station, CE; "Soil Pressure Cell Investigation"; Technical Memorandum No. 210-1, July 1944; Vicksburg, Miss.; Unclassified.

3. D. H. Trollope and D. T. Currie; "Small Embedded Earth Pressure Cells - Their Design and Calibration"; Proceedings of the Third Australia-New Zealand Conference on Soil Mechanics and Foundation Engineering, August 1960, Pages 145-151; University of Sydney, N.S.W., Australia; Unclassified.

4. K. R. Peattie and R. W. Sparrow; "The Fundamental Action of Earth Pressure Cells"; Journal of the Mechanics and Physics of Solids, 1954, Vol 2, Pages 141-155; London, England; Unclassified.

5. D. W. Taylor; "Review of Pressure Distribution Theories, Earth Pressure Cell Investigations and Pressure Distribution Data"; Contract Report No. W22-053-eng-185, November 1945; Massachusetts Institute of Technology, Cambridge, Mass.; Unclassified.

6. G. E. Monfore; "Analysis of the Stress Distributions in and Near Stress Gages Embedded in Elastic Solids"; Structural Research Laboratory Report No. SP-26, June 1950; U. S. Department of the Interior, Bureau of Reclamation, Research and Geology Division, Denver, Colorado; Unclassified.

7. A. C. Whiffin and S. A. H. Morris; "Piezoelectric Gauge for Measuring Dynamic Stresses Under Roads"; The Engineer, April 1962, Vol. 213, Pages 741-746; Morgan Bros. Limited, London, England; Unclassified.

8. G. Plantema; "A Soil Pressure Cell and Calibration Equipment"; Proceedings of the Third International Conference on Soil Mechanics and Foundation Engineering, August 1953, Vol. 1, Pages 283-298; Zurich, Switzerland; Unclassified.

9. C. W. Bert and N. A. Crites; "Experimental Mechanics in the Development of a New Miniature Pressure Transducer"; Experimental Mechanics, Proceedings of the First International Congress on Experimental Mechanics, 1963, Pages 307-322; The Macmillan Co., New York, N. Y.; Unclassified.

10. S. Timoshenko and S. Woinowsky-Krieger; "Theory of Plates and Shells"; Second Edition, 1959, Pages 51-73; McGraw-Hill Book Company, Inc., New York, N. Y.; Unclassified.

11. C. C. Perry and H. R. Lissner; "The Strain Gage Primer"; Second Edition, 1962; McGraw-Hill Book Company, Inc., New York, N. Y.; Unclassified.

12. J. K. Ingram; "Procedure for Assembling SE-Type Soil Stress Gages"; Instruction Report No. 8, March 1967; U. S. Army Engineer Waterways Experiment Station, CE, Vicksburg, Miss.; Unclassified.

13. J. K. Ingram; "Development of a Free-Field Soil Stress Gage for Static and Dynamic Measurement, Instruments and Apparatus for Soil and Rock Mechanics"; STP 392, June 1965; American Society for Testing and Materials, Philadelphia, Pa.; Unclassified.

14. G. E. Albritton; "Description, Proof Testing, and Evaluation of the Blast Load Generator Facility"; Technical Report No. 1-707, December 1965; U. S. Army Engineer Waterways Experiment Station, CE, Vicksburg, Miss.; Unclassified.

15. P. F. Hadala; "Sidewall Friction Reduction in Static and Dynamic Small Blast Load Generator Tests"; U. S. Army Engineer Waterways Experiment Station, CE, Vicksburg, Miss.; In preparation; Unclassified.

16. P. F. Hadala; "The Effect of Placement Method on the

Response of Soil Stress Gages"; Technical Report No. 3-803, November 1967; U. S. Army Engineer Waterways Experiment Station, CE, Vicksburg, Miss.; Unclassified.

17. P. A. Abbot; "Effects of Boundary Friction on Transmission of Static Stress Through Sand in Cylindrical Tanks"; Draft Report, August 1964; Air Force Weapons Laboratory, Kirtland Air Force Base, New Mexico; Unclassified.

18. J. V. Zaccor and others; "Study of the Dynamic Stress-Strain and Wave Propagation Characteristics of Soils; Concepts of Shock Behavior in a Granular Media"; Contract Report No. 3-91, Report 4, March 1965; U. S. Army Engineer Waterways Experiment Station, CE, Vicksburg, Miss.; Report prepared by United Research Services, Inc., Burlingame, Calif.; Unclassified.

19. N. M. Newmark and J. D. Haltiwanger; "Air Force Design Manual, Principles and Practices for Design of Hardened Structures"; Technical Documentary Report No. AFSWC-TDR-62-138, December 1962, Chapter 4, Pages 1-90; Air Force Special Weapons Center, Kirtland Air Force Base, New Mexico; Unclassified.

20. J. M. Dewey; "Precursor Shocks Produced by a Large Yield TNT Explosion"; Special Publication 46, March 1965; Suffield

Experimental Station, Ralston, Alberta, Canada; Lnclassified.

21. J. G. Jackson, Jr., and P. F. Hadala; "Dynamic Bearing
Capacity of Soils; The Application of Similitude to Small-Scale
Footing Tests"; Technical Report No. 3-599, Report 3, December 1964;
U. S. Army Engineer Waterways Experiment Station, CE, Vicksburg,
Miss.; Unclassified.

DOCUMENT CONTROL DATA - R & D

(Security classification of title, body of abstract and indexing annotation must be entered when the overall report is classified)

1. ORIGINATING ACTIVITY *(Corporate author)*	2a. REPORT SECURITY CLASSIFICATION
U. S. Army Engineer Waterways Experiment Station Vicksburg, Miss.	Unclassified
	2b. GROUP

3. REPORT TITLE

DEVELOPMENT OF A FREE-FIELD SOIL STRESS GAGE FOR STATIC AND DYNAMIC MEASUREMENTS

4. DESCRIPTIVE NOTES *(Type of report and inclusive dates)*
Final report

5. AUTHOR(S) *(First name, middle initial, last name)*

James K. Ingram

6. REPORT DATE	7a. TOTAL NO. OF PAGES	7b. NO. OF REFS
February 1968	112	22
8a. CONTRACT OR GRANT NO.	9a. ORIGINATOR'S REPORT NUMBER(S)
b. PROJECT NO.	Technical Report No. 1-814
c. NWET Subtask 13.503A	9b. OTHER REPORT NO(S) (Any other numbers that may be assigned this report)
d.	

10. DISTRIBUTION STATEMENT

This document has been approved for public release and sale; its distribution is unlimited.

11. SUPPLEMENTARY NOTES	12. SPONSORING MILITARY ACTIVITY
	Defense Atomic Support Agency Washington, D. C.

13. ABSTRACT   This report describes the development of three free-field stress gage types. One gage design, the sand dollar gage, was abandoned early in the investigation, while the other two, the W and SE gages, were subjected to various evaluation tests. Static and dynamic tests in sand and clay were conducted in the Small Blast Load Generator (SBLG). The gages have been used in the laboratory evaluation of a cold gas loader and in two field tests. Evaluation of the performance of the gages in these tests is presented in Appendix A. The gage placement techniques used in the SBLG tests are described in Appendix B. The gages are rugged and relatively easy to place in the laboratory. They may be used for both static and dynamic measurements and have a linear pressure range from 1 to above 1,800 psi. The gages have very low acceleration sensitivity and hysteresis, and have excellent dynamic response capability. Their temperature sensitivity is such that it will be of little consequence in dynamic tests and can be corrected for in long-term static tests. Electrical sensitivity remains essentially constant from -30 to 150 F. Of the two gage types discussed, the SE gage is recommended for use. It is much easier to place, is more rugged, and produces a cleaner dynamic signal than the W gage. The gages can be calibrated to compensate for registration errors due to differences in soil and gage modulus; however, gage registration was found to be a function of placement method, depth of burial, input pressure, and conditions of the medium, not simply of modulus ratio. Where a minimum number of gages are to be used in sand, a dense tamping-in placement method is recommended for use in laboratory tests. For tests in clay, the cut/no-cover method, in which the gage is placed flush with the clay surface and covered in normal lifts, is recommended. Further investigation of field placement techniques is recommended.

DD FORM 1473

14. KEY WORDS	LINK A		LINK B		LINK C	
	ROLE	WT	ROLE	WT	ROLE	WT
Soil stress gages						

114